BAZ2A-RNA mediated association with TOP2A and KDM1A represses genes implicated in prostate cancer

Marcin Roganowicz[1,2], Dominik Bär[1], Cristiana Bersaglieri[1], Rossana Aprigliano[1] and Raffaella Santoro[1*]

1. Department of Molecular Mechanisms of Disease, DMMD, University of Zurich, 8057 Zurich, Switzerland
2. RNA Biology Program, Life Science Zurich Graduate School, University of Zurich, 8057 Zurich, Switzerland

* Corresponding author:

Raffaella Santoro (raffaella.santoro@dmmd.uzh.ch)

Abstract

BAZ2A is the repressor of rRNA genes that are transcribed by RNA Polymerase I. In prostate cancer (PCa), however, BAZ2A function goes beyond this role since it can also repress other genes that are frequently silenced in metastatic disease. However, the mechanisms of BAZ2A-mediated repression in PCa remain elusive. Here we show that BAZ2A represses genes implicated in PCa through its RNA-binding TAM domain using mechanisms differing from rRNA gene silencing. While TAM domain mediates BAZ2A recruitment to rRNA genes, in PCa cells this is not required for BAZ2A association with target genes. Instead, BAZ2A-TAM domain in association with RNA mediates the interaction with topoisomerase 2A (TOP2A) and histone demethylase KDM1A, whose expression positively correlates with BAZ2A levels in both localized and aggressive PCa. Pharmacological inhibition of TOP2A and KDM1A activities upregulates the expression of BAZ2A-repressed genes that are regulated by a class of inactive enhancers bound by BAZ2A whereas rRNA genes are not affected. Our findings showed a novel RNA-based mechanism of gene regulation in PCa. Further, the data indicate that RNA-mediated interactions between BAZ2A and TOP2A and KDM1A repress genes critical to PCa and may prove to be useful to stratify prostate cancer risk and treatment in patients.

Introduction

Prostate cancer (PCa) is the second most frequent cancer in men and the fifth leading cause of cancer death (Sung et al., 2021). Most of the PCa are indolent ones, with no threat to mortality, however, in many cases an aggressive form of disease develops and progresses to metastasis, which accounts for almost two thirds of prostate cancer-related deaths (Siegel et al., 2015). PCa displays a high heterogeneity that leads to distinct histopathological and molecular features (Li and Shen, 2018). This heterogeneity posits one of the most confounding and complex factors underlying its diagnosis, prognosis, and treatment (Yadav et al., 2018).

BAZ2A (also known as TIP5) is a chromatin repressor known for its role in the silencing of rRNA genes, which are transcribed by the RNA Polymerase I (Pol I) (Guetg et al., 2010; Santoro et al., 2002). Recent studies showed that BAZ2A is also implicated in several cancers such as PCa and hepatocellular carcinoma (Gu et al., 2015; Li et al., 2018). In the case of PCa, it was shown that BAZ2A function goes beyond the regulation of rRNA genes and is implicated in aggressive disease (Gu et al., 2015; Peña-Hernández et al., 2021; Pietrzak et al., 2020). BAZ2A is highly expressed in metastatic PCa and involved in maintaining PCa cell growth by repressing genes frequently silenced in metastatic PCa (Gu et al., 2015; Peña-Hernández et al., 2021). Moreover, elevated BAZ2A level indicates poor outcome (Pietrzak et al., 2020) and is also of high prognostic value for predicting PCa recurrence (Gu et al., 2015). However, the mechanisms of how BAZ2A mediates gene repression in PCa remain yet elusive.

BAZ2A contains a RNA-binding domain known as TAM (TIP5/ARBD/MBD). The TAM domain plays a key role in rRNA gene silencing through the interaction with the long non-coding (lnc) promoter (p)RNA, a transcript originating from an alternative promoter of the rRNA genes (Anosova et al., 2015; Guetg et al., 2012; Mayer et al., 2006). The association of BAZ2A-TAM domain with pRNA is required for the interaction with the transcription termination factor I (TTF1) that mediates BAZ2A recruitment to rRNA genes and transcriptional repression (Leone et al., 2017; Savic et al., 2014). However, it remains yet to elucidate whether BAZ2A uses similar RNA-mediated mechanisms to repress genes implicated in aggressive PCa.

In this work, we show that BAZ2A represses genes in PCa through its RNA-binding TAM domain using mechanisms that substantially differ from the ones used to silence rRNA genes. We found that rRNA gene expression in PCa cells is still affected by pRNA and BAZ2A,

indicating that PCa cells retain similar mechanisms to establish rRNA gene silencing that were described in non-cancer cells (Guetg et al., 2010; Leone et al., 2017; Mayer et al., 2006). In contrast, the other BAZ2A-regulated genes in PCa do not depend on pRNA. Further, BAZ2A-TAM domain is not required for the recruitment to its target genes. Instead, TAM domain mediates BAZ2A association with factors implicated in the regulation of gene expression, chromatin organization, nuclear pore complex, and RNA splicing. Among BAZ2A-TAM dependent interacting proteins we found topoisomerase 2A (TOP2A) and histone demethylase KDM1A, which have been previously implicated in aggressive PCa (Labbé et al., 2017; Liang et al., 2017; Sehrawat et al., 2018). Importantly, BAZ2A-TAM mediated interaction with TOP2A and KDM1A requires RNA. TOP2A and KDM1A expression levels positively correlate with BAZ2A levels in both localized and aggressive PCa. Moreover, the repression of BAZ2A-TAM dependent genes correlates with primary and metastatic tumours with high BAZ2A, KDM1A, and TOP2A content. Finally, pharmacological inhibition of TOP2A and KDM1A activity specifically upregulates the expression of BAZ2A-TAM repressed genes that are regulated by a class of inactive enhancers bound by BAZ2A. In contrast, the expression of rRNA genes was not affected by TOP2A and KDM1A inhibition, highlighting different BAZ2A-mediated repressive mechanisms that depend on the gene context. Our findings showed a novel RNA-based mechanism of gene regulation in PCa. Further, the data indicate that RNA-mediated interactions between BAZ2A and TOP2A and KDM1A regulate genes critical to PCa and may prove to be useful for the stratification of prostate cancer risk and treatment in patients.

Results

BAZ2A-TAM domain mediates BAZ2A-RNA interaction in PC3 cells

Previous results showed that the function of BAZ2A in PCa goes beyond the silencing of rRNA genes since it can also repress other genes that are linked to aggressive PCa (Gu et al., 2015; Peña-Hernández et al., 2021). In BAZ2A-mediated rRNA gene silencing, BAZ2A-TAM domain plays an important role since its interaction with the lncRNA pRNA is required for BAZ2A recruitment to the promoter of rRNA genes (Leone et al., 2017; Mayer et al., 2006; Savic et al., 2014). To determine whether in PCa cells BAZ2A represses genes other than rRNA genes using similar mechanisms required for the establishment of rRNA gene silencing, we analysed

the role of BAZ2A-TAM domain in PCa cells. We first investigated whether BAZ2A can interact with RNA in PCa cells. We irradiated metastatic PCa PC3 cells with ultraviolet (UV) light that promotes the formation of covalent bonds between RNA binding proteins (RBPs) and their direct RNA binding sites (Lee and Ule, 2018) (**Fig. 1A**). We performed HA-immunoprecipitation (IP) using a previously established PC3 cell line that expresses endogenous BAZ2A tagged with FLAG-HA (H/F-BAZ2A$_{end}$-PC3) (Peña-Hernández et al., 2021) followed by ^{32}P-radiolabelling of RNA (**Fig. 1A**). As control, we performed HA-IPs with F/H-BAZ2A-PC3 cells that were not UV-irradiated and crosslinked parental PC3 cells. Although similar amounts of H/F-BAZ2A were immunoprecipitated from UV crosslinked and not crosslinked F/H-BAZ2A$_{end}$-PC3 cells, radioactive RNA signal could only be detected from UV-irradiated F/H-BAZ2A$_{end}$ cells. This signal was reduced upon treatment with high RNase I amount, indicating that BAZ2A directly interacts with RNA in PC3 cells. To determine whether the interaction with RNA is mediated by the RNA-binding BAZ2A-TAM domain, we performed HA-immunoprecipitation with UV-irradiated PC3 cells transfected with plasmids expressing H/F-BAZ2A wild-type (WT) or -BAZ2A$_{WY/GA}$ mutant that previous work showed to have a reduced binding affinity for RNA (Anosova et al., 2015; Guetg et al., 2012; Mayer et al., 2006) (**Fig. 1B**). We found that immunoprecipitated BAZ2A$_{WT}$ displays a stronger RNA radioactive signal compared to BAZ2A$_{WY/GA}$, indicating that BAZ2A-RNA interaction in PC3 cells occurs through BAZ2A-TAM domain. Taken together, these results indicate that in PCa cells the TAM domain is required for BAZ2A interaction with RNA. Next, we tested whether pRNA, the known BAZ2A-intercating RNA (Mayer et al., 2006), could affect the expression of known BAZ2A-repressed genes in PCa cells (Gu et al., 2015). We measured the expression of validated BAZ2A target genes that were found in our previous studies to be bound and repressed by BAZ2A in PC3 cells and frequently silenced in metastatic PCa (Gu et al., 2015; Pena-Hernandez et al., 2021). To determine the role of pRNA for the regulation of these BAZ2A-repressed genes, we co-transfected PC3 cells with constructs expressing RNA-control or pRNA sequences under the control of the human rRNA gene promoter and GFP under the control of EF-1α promoter, and isolated GFP(+)-cells by FACS sorting 72 hours later (**Fig. 1C**). Consistent with previous results, the overexpression of pRNA caused downregulation of 45S pre-rRNA, indicating that pRNA downregulates rRNA gene expression in PCa cells as well (Mayer et al., 2006) (**Fig. 1D**). In contrast, pRNA did not

cause significant changes in the expression of the other known BAZ2A-repressed genes (Gu et al., 2015), suggesting that their regulation is pRNA independent. These results suggest that BAZ2A represses these genes using mechanisms that differ from the silencing of rRNA genes that requires pRNA.

BAZ2A regulates a set of genes involved in PCa through its TAM domain

To determine whether BAZ2A-mediated gene regulation in PCa cells depends on the TAM domain, we performed RNAseq analysis on PC3 cells expressing $BAZ2A_{WT}$ and $BAZ2A_{\Delta TAM}$. We engineered all-in-one constructs that express F/H-tagged mouse $BAZ2A_{WT}$ (F/H-$mBAZ2A_{WT}$) or $BAZ2A_{\Delta TAM}$ (F/H-$mBAZ2A_{\Delta TAM}$) under CMV promoter, the GFP reporter gene under EF-1α promoter, and shRNA against human (h)BAZ2A sequences that do not target m*BAZ2A* (**Fig. 2A**). hBAZ2A and mBAZ2A share high sequency homology (86%) and identical TAM domain sequences. The expression of shRNA that specifically targets hBAZ2A was reasoned to obtain the expression of ectopic $mBAZ2A_{WT}$ and $mBAZ2A_{\Delta TAM}$, allowing simultaneous downregulation of the endogenous hBAZ2A. We transfected PC3 cells with the all-in-one constructs and isolated GFP(+)-cells by FACS sorting 72 hours later. We confirmed equal expression of $mBAZ2A_{WT}$ and $mBAZ2A_{\Delta TAM}$ by western blot (**Fig. 2B**) and the reduction of endogenous hBAZ2A by qRT-PCR in FACS-sorted GFP(+) PC3 cells (**Fig. 2C**). As expected, due to transient transfection, the expression of ectopic mBAZ2A was higher than endogenous hBAZ2A. Correlation analysis clustered separately PCa cells expressing $mBAZ2A_{\Delta TAM}$ or $mBAZ2A_{WT}$, indicating a differential gene expression profile (**Supplementary Fig. S1**). We identified 123 upregulated genes and 553 downregulated genes in PC3 cells expressing $mBAZ2A_{\Delta TAM}$ compared to cells expressing $mBAZ2A_{WT}$ ($\log_2$ fold change ±0.58, $P < 0.05$, **Fig. 2D**). The top GO terms for the upregulated genes were related to tissue and organ development, cell migration and locomotion, regulation of epithelial cells proliferation, and angiogenesis (**Fig. 2E**). Many of these processes are recognized as hallmarks of cancer, such as proliferative signalling, angiogenesis induction, and activation of invasion and metastasis (Hanahan and Weinberg, 2011; Zhong et al., 2020). The GO terms for downregulated genes were mostly related to metabolic processes that are also known to contribute to various cancers development by fuelling cancer cells growth and division (Hanahan and Weinberg, 2011).

Next, we used published RNAseq data (Peña-Hernández et al., 2021) to define differentially expressed genes in PC3 cells depleted of BAZ2A by siRNA (BAZ2A-regulated genes; $\log_2$ fold change ±0.58, $P < 0.05$) and asked how many BAZ2A-regulated genes were significantly affected by $BAZ2A_{\Delta TAM}$ expression (**Fig. 2F**). We found that 36% and 26% of upregulated and downregulated genes upon BAZ2A-knockdown (KD) respectively were significantly affected by $BAZ2A_{\Delta TAM}$ expression. Remarkably, the majority of these BAZ2A-regulated genes showed similar changes in gene expression upon the expression of $BAZ2A_{\Delta TAM}$. A large portion (74%) of these genes upregulated upon BAZ2A-KD were significantly upregulated upon the expression of $BAZ2A_{\Delta TAM}$. Similarly, 69% of gene downregulated upon BAZ2A-KD were also downregulated by $BAZ2A_{\Delta TAM}$. These results suggest a major role of BAZ2A-TAM domain in affecting BAZ2A-regulated gene expression in PCa cells. We further supported these results by measuring through qRT-PCR the expression of validated BAZ2A-repressed genes in PCa (Gu et al., 2015) that did not depend on pRNA (**Fig. 1D**) and found that they were significantly upregulated in cells expressing $BAZ2A_{\Delta TAM}$ compared to PC3 cells expressing $BAZ2A_{WT}$ or only GFP (**Fig. 2G**). These results indicated that the repression of these BAZ2A-repressed genes is dependent on BAZ2A-TAM domain but pRNA independent. We did not observe any evident additional downregulation upon $mBAZ2A_{WT}$ expression, suggesting that these genes are already repressed by BAZ2A and cannot be further downregulated by increasing BAZ2A expression levels. Taken together, these results point for a role of BAZ2A in the regulation of the expression of genes implicated in cancer-related processes through its TAM domain.

BAZ2A-TAM domain is required for the repression of a set of genes that have their enhancers bound by BAZ2A

Previous BAZ2A-ChIPseq analyses in PC3 cells determined that BAZ2A associates with a class of inactive enhancers that are enriched in histone H3 acetylated at Lysin 14 (H3K14ac) and depleted of H3K27ac and H3K4me1 (Peña-Hernández et al., 2021) (**Fig. 3A**). This group of inactive enhancers was termed class 2 (C2)-enhancers and appears to be the major mechanism of BAZ2A-regulation in PCa cells since only few BAZ2A-regulated genes had their promoter associated with BAZ2A (Peña-Hernández et al., 2021). The interaction of BAZ2A with C2-enhancers was shown to be mediated by the BAZ2A-bromodomain that specifically binds

to H3K14ac. BAZ2A-bound C2-enhancers are significantly enriched in H3K14ac and the repressive mark H3K27me3 and depleted of the active modification H3K27ac relative to the active enhancer class C1 marked by H3K27ac, H3K4me1, and DNase I hypersensitive sites (Peña-Hernández et al., 2021) and C2-enhancers not bound by BAZ2A (**Fig. 3B**). Importantly, genes in the nearest linear proximity to BAZ2A-bound C2-enhancers were found to be repressed by BAZ2A, indicating that BAZ2A could repress genes through the association with this class of inactive enhancers. To determine whether BAZ2A-TAM domain is required for the repression of these genes, we analysed the RNAseq profiles of PC3 cells expressing $BAZ2A_{WT}$ and $BAZ2A_{\Delta TAM}$ and found that 25% (240) of the genes in the nearest linear proximity to BAZ2A-bound C2-enhancers were significantly affected by $BAZ2A_{\Delta TAM}$ compared to $BAZ2A_{WT}$ (**Fig. 3A,C,D**). Remarkably, the majority of these BAZ2A-TAM regulated genes (202, 84%) were significantly upregulated upon the expression of $BAZ2A_{\Delta TAM}$, suggesting a major role of BAZ2A-TAM domain in repressing gene transcription through its interaction with C2-enhancers. These results also suggest that genes downregulated upon the expression of $BAZ2A_{\Delta TAM}$ (**Fig. 2E**) might not be direct targets of BAZ2A and are probably affected through indirect mechanisms. The top GO terms of genes repressed through BAZ2A-TAM domain were linked to signal transduction, response to wounding, and cell migration and motility (**Fig. 3E**). Interestingly, the analysis of a comprehensive dataset comparing gene expression between metastatic tumours to normal tissue (Chandran et al., 2007; Yu et al., 2004) showed that many genes upregulated by $BAZ2A_{\Delta TAM}$ and implicated in signal transduction and cell motility are repressed in metastatic PCa (**Supplementary Fig. S2**).

Since the TAM domain was shown to be required for BAZ2A association with rRNA genes (Mayer et al., 2006), we asked whether this was also the case for BAZ2A interaction with C2-enhancers. We performed ChIP analysis of PC3 cells transfected with F/H-$mBAZ2A_{WT}$ or F/H-$mBAZ2A_{\Delta TAM}$ and analysed BAZ2A association with BAZ2A-bound C2-enhancers that were close to genes upregulated by $BAZ2A_{\Delta TAM}$. However, we did not find any significant alterations in the binding of $BAZ2A_{\Delta TAM}$ with these regions relative to $BAZ2A_{WT}$ (**Fig. 3F**). Similarly, the interaction with the promoter of *AOX1*, a known gene directly regulated by BAZ2A (Gu et al., 2015; Peña-Hernández et al., 2021) was not affected. These results indicate that the interaction with these loci is not mediated by BAZ2A-TAM domain. Further, they support previous data

showing that it is the BAZ2A-BRD domain to be required for the interaction of C2-enhancers that contain H3K14ac (Peña-Hernández et al., 2021). Consistent with previous results (Mayer et al., 2006), the ChIP analysis showed that the association of BAZ2A$_{\Delta TAM}$ with the promoter of rRNA genes was reduced compared to BAZ2A$_{WT}$ (**Fig. 3F**). Thus, while for rRNA gene silencing BAZ2A-TAM is required for the association with chromatin, in the case of the other BAZ2A-regulated genes, BAZ2A-TAM domain is not necessary for the recruitment to target loci, suggesting different mechanisms by which BAZ2A represses gene expression in PCa cells.

BAZ2A associates with KDM1A and TOP2A in a TAM domain and RNA dependent manner

We hypothesized that BAZ2A-TAM domain and its ability to interact with RNA might be important for the association with factors implicated in BAZ2A-mediated gene repression in PCa cells. To test this, we performed HA-IP combined with mass-spec analysis from PC3 cells transfected with plasmids expressing F/H-BAZ2A$_{WT}$ or the deficient RNA-binding mutant F/H-BAZ2A$_{WY/GA}$. In this series of experiments, we reasoned to use BAZ2A$_{WY/GA}$ instead of BAZ2A$_{\Delta TAM}$ mutant to obtain a more specific identification of proteins requiring RNA to interact with BAZ2A. The IP specificity was validated by western blot with antibodies against HA to detect F/H-BAZ2A and against SNF2H, a well-known BAZ2A-interacting protein (Dalcher et al., 2020; Strohner et al., 2001) (**Fig. 4A**). We defined as BAZ2A$_{WT}$-interacting proteins those factors showing in all the three replicates at least two peptides and ≥ 2 fold peptide number in IPs with H/F-BAZ2A$_{WT}$ relative to IPs from cells transfected with empty vector. To identify factors that specifically associate with BAZ2A through a functional BAZ2A-TAM domain, we considered BAZ2A$_{WT}$-intercating proteins that showed ≥ 2 fold peptide number in BAZ2A$_{WT}$-IPs relative to BAZ2A$_{WY/GA}$-IPs in at least two independent replicates (**Fig. 4B**). Using these criteria, proteins previously shown to interact with BAZ2A independently of RNA, such as SNF2H and DHX9, showed similar binding with both BAZ2A$_{WT}$ and BAZ2A$_{WY/GA}$ (Leone et al., 2017) (**Fig. 4B**). We identified 74 proteins that had decreased association with BAZ2A$_{WY/GA}$ compared to BAZ2A$_{WT}$. We applied the Search Tool for the Retrieval of Interacting Genes/Proteins database (STRING) (Szklarczyk et al., 2015) and found that proteins with decreased association with BAZ2A$_{WY/GA}$ were involved in pathways linked to the regulation of gene expression,

chromosome organization, nuclear pore complex organization, and RNA processing (**Fig. 4C**). Among them, we found factors that regulate transcription and topological states of DNA such as topoisomerase 2A and 2B (TOP2A and TOP2B), histone demethylase KDM1A (also known as LSD1) and several components of cohesin protein complex (SMC1A, RAD21, STAG2). We also observed loss of BAZ2A interactions with factors involved in RNA processing and splicing (CTNNBL1, EFTUD2) and nuclear pore complex formation (NUP107, NUP133, NUP97). We validated the dependency of BAZ2A-TAM domain for BAZ2A-interaction with TOP2A, SMC1A, RAD21, NUP107, and KDM1A by anti-HA IP of PC3 cells transfected with plasmids expressing H/F-mBAZ2A$_{WT}$, -mBAZ2A$_{WY/GA,}$ and -mBAZ2A$_{\Delta TAM}$ followed by western blot (**Fig. 4D**). We confirmed these interactions also with endogenous BAZ2A by performing HA-IP in PC3 cells expressing endogenous BAZ2A tagged with HA and FLAG sequences (H/F-BAZ2A$_{end}$) (**Fig. 4E**). To determine whether these BAZ2A-interactions are mediated by the TAM domain itself or RNA bound to the TAM domain, we treated nuclear extracts of F/H-BAZ2A-PC3 cells and parental PC3 cells with RNase A and found that TOP2A and KDM1A association with BAZ2A was strongly reduced (**Fig. 4E**). In contrast, BAZ2A-association with RAD21, SMC1A, and NUP107 were not clearly affected by RNase A, suggesting that these interactions are BAZ2A-TAM-dependent but RNA independent. These results indicated that BAZ2A-TAM domain mediates alone or in combination with RNA the interaction with proteins mainly involved in chromatin regulation. Further, the data show that RNA may act as a scaffold for the association of BAZ2A with TOP2A and KDM1A (**Fig. 4F**).

KDM1A and TOP2A correlate with gene expression in PCa through BAZ2A-TAM domain

Previous studies have implicated an involvement of both TOP2A and KDM1A in PCa. Elevated expression of KDM1A was shown to correlate with PCa recurrence (Kahl et al., 2006; Kashyap et al., 2013). Further, high TOP2A levels were significantly associated with increased risk of systemic progression in PCa patients (Cheville et al., 2008). Consistent with these results, the analyses of two data sets comparing normal tissue, localized tumor, and metastatic PCa (Chandran et al., 2007; Varambally et al., 2005; Yu et al., 2004) revealed that *TOP2A* levels are highly elevated in metastatic PCa (**Fig. 5A,B**). This pattern is very similar to *BAZ2A* expression levels that previous work also detected to be high in metastatic PCa relative to

normal tissue and localized tumours (Gu et al., 2015). In contrast, the expression of *KDM1A* between metastatic PCa relative to localized tumor and normal tissue were less consistent between the two different datasets. However, the analysis of a large cohort of primary PCa and metastatic castration resistant PCa (CRPC) (333 and 118 tumours, respectively) (Cancer Genome Atlas Research, 2015; Robinson et al., 2015) revealed a significant positive correlation of both TOP2A and KDM1A levels with BAZ2A expression in both metastatic and primary tumors (**Fig. 5C-F**). Furthermore, the majority of primary PCas with high levels of *TOP2A* or *KDM1A* belonged to the PCa subtype characterized by copy number alterations of the tumor suppressor gene *PTEN* and containing ERG fusion, which is the subtype characterizing PCa with high BAZ2A expression (Pietrzak et al., 2020) (**Fig. 5G**). These results suggest that TOP2A and KDM1A might be functionally related to BAZ2A for the regulation of gene expression in PCa. To test this hypothesis, we analysed the expression of BAZ2A-TAM repressed genes (i.e., upregulated upon $BAZ2A_{\Delta TAM}$ expression in PC3 cells) and its connection to KDM1A and TOP2A using transcriptomic dataset from a large cohort of primary PCa (Cancer Genome Atlas Research, 2015). First, we classified tumours with high and low BAZ2A levels (83 primary PCas for each group, $BAZ2A^{high}$, the top 25% of PCas with the highest BAZ2A expression; $BAZ2A^{low}$, the top 25% of PCas with the lowest BAZ2A expression) and identified 409 genes that were significantly downregulated in $BAZ2A^{high}$ compared to $BAZ2A^{low}$ tumours (**Fig. 6A**). We found that 28% (113) of these genes were BAZ2A-TAM repressed genes in PC3 cells. Importantly, 74% of these BAZ2A-TAM dependent genes (84) were significantly downregulated by comparing $BAZ2A^{high}$/$KDM1A^{high}$ tumours (i.e., 39 PCas that scored as the top 25% with the highest BAZ2A and KDM1A expression, respectively) compared to $BAZ2A^{low}$/$KDM1A^{low}$ tumours (41 PCas) (**Fig. 6A,B, Supplementary Fig. S3A**). The rest of genes not showing statistical significance were also downregulated upon treatment with KDM1Ai, except for two genes that were upregulated (**Fig. 6B**). We repeated a similar analysis for TOP2A and found that 90% (102) of genes repressed by BAZ2A-TAM in PC3 cells and downregulated in primary $BAZ2A^{high}$ PCas were also downregulated in $BAZ2A^{high}$/$TOP2A^{high}$ tumours compared to $BAZ2A^{low}$/$TOP2A^{low}$ (**Fig. 6C,D, Supplementary Fig. S3B**). Moreover, the majority of these BAZ2A-TAM regulated genes were downregulated in both $BAZ2A^{high}$/$KDM1A^{high}$ and $BAZ2A^{high}$/$TOP2A^{high}$ (**Fig. 6D**). This is result is also consistent with the fact that about 50% of

BAZ2A^{high}/KDM1A^{high} and BAZ2A^{high}/TOP2A^{high} correspond to tumours with high TOP2A and KDM1A expression levels, respectively (Q1) (**Supplementary Fig. S3C**). Gene ontology terms of these genes correspond to metabolic and wound healing related processes, which are very similar to the terms found for BAZ2A$_{\Delta TAM}$-regulated genes in PC3 cells (**Supplementary Fig. S3D**). Next, we analysed a dataset comparing metastatic PCa to normal and primary tumours (Chandran et al., 2007; Yu et al., 2004). We found that a large fraction (44%) of these BAZ2A-TAM regulated genes downregulated in BAZ2A^{high}/KDM1A^{high} or BAZ2A^{high}/TOP2A^{high} primary PCa were significantly repressed in metastatic PCa compared to normal and primary tumours (44% and 47%, respectively) whereas only few were upregulated (6% and 8%) (**Fig. 6F,G**). Gene ontology terms of these genes correspond to developmental and wound healing related processes (**Supplementary Fig. S3E**). Taken together, these results suggest an important link between BAZ2A-TAM domain, KDM1A, and TOP2A in the regulation of genes linked to PCa.

Inhibition of KDM1A and TOP2A affects BAZ2A-TAM repressed genes in PCa cells

To determine whether pharmacological inhibition of KDM1A and TOP2A affects the expression of genes regulated by BAZ2A-TAM domain, we treated PC3 cells with the KDM1A inhibitor OG-L002 (KDM1Ai) or the TOP2A inhibitor ICR-193 (TOP2Ai) (Ishida et al., 1991) and perform RNAseq analyses. In the case of KDM1A inhibition, we identified 453 upregulated genes and 152 downregulated genes in PC3 cells treated with KDM1Ai compared to control cells ($\log_2$ fold change ±0.58, $P < 0.05$, **Fig. 7A**). Gene ontology term analysis revealed that the upregulated genes are implicated in pathways linked to development whereas downregulated genes are linked to defence response processes (**Fig. 7B**). Next, we asked whether BAZ2A-TAM regulated genes were also regulated by KDM1A. We found that 32% and 26% of genes respectively upregulated or downregulated by BAZ2A$_{\Delta TAM}$ expression were also significantly affected by KDM1Ai treatment (**Fig. 7C, Supplementary Fig. S4A**). Importantly, the majority of these BAZ2A-TAM regulated genes affected by KDM1Ai treatment showed similar changes upon the expression of BAZ2A$_{\Delta TAM}$ and treatment with KDM1Ai. Genes upregulated by BAZ2A$_{\Delta TAM}$ and KDM1Ai in PC3 cells included all the 84 BAZ2A-TAM repressed genes that were downregulated in BAZ2A^{high}/KDM1A^{high} primary PCa (**Fig.6A, 7D**), suggesting an important role of KDM1A activity in BAZ2A-TAM dependent gene regulation in PCa.

Next, we analysed the effect of TOP2A inhibition with TOP2Ai ICR-193. We identified 722 upregulated genes and 410 downregulated genes in PC3 cells treated with TOP2Ai compared to control cells ($\log_2$ fold change ±0.58, $P < 0.05$, **Fig. 7E**). Gene ontology term analysis revealed that downregulated genes were strongly implicated in cell cycle progress and chromosome segregation, an expected result given the known role of TOP2A in these processes (Chen et al., 2015) (**Fig. 7F**). We asked whether BAZ2A-TAM regulated genes were also regulated by TOP2A and found that 52% and 35% of genes significantly upregulated or downregulated by $BAZ2A_{\Delta TAM}$ expression were also significantly affected by TOP2Ai treatment (**Fig. 7G, Supplementary Fig. S4B**). In the case of genes upregulated by $BAZ2A_{\Delta TAM}$ in PC3 cells, 52% of them were significantly upregulated by TOP2Ai treatment and included 52 out of the 102 BAZ2A-TAM repressed genes that were downregulated in $BAZ2A^{high}$/$TOP2A^{high}$ primary PCa (**Fig. 6C,7H**). Moreover, about half of these BAZ2A-TAM and TOP2Ai upregulated genes were also significantly regulated by treatment with KDM1Ai and the majority of them were upregulated (**Fig. 7I**). We observed similar results for genes downregulated by TOP2Ai (**Supplementary Fig. S4B**). These results further indicate that KDM1A and TOP2A are implicated in BAZ2A-TAM regulated gene repression in PCa. Importantly, measurements of 45S pre-rRNA levels upon treatment with KDM1Ai or TOP2Ai revealed no significant changes, underscoring distinct mechanisms of BAZ2A repression in PCa cells based on the dependency of TOP2A and KDM1A (**Fig. 7J**).

Finally, we asked how many BAZ2A-TAM-regulated genes that are located in the nearest linear proximity to BAZ2A-bound C2-enhancers were affected by the treatment of PC3 cells with KDM1Ai or TOP2Ai (**Fig. 8**). More than one third (39%) of genes upregulated upon $BAZ2A_{\Delta TAM}$ expression were significantly affected by KDM1Ai and the majority (77%) show similar changes to $BAZ2A_{\Delta TAM}$ expression, being upregulated compared to control cells (**Fig. 8A**). These results indicate that KDM1A activity is implicated in the repression of genes having their corresponding C2-enhancers bound by BAZ2A and repressed through BAZ2A-TAM domain. In the case of TOP2A inhibition, we found that 52% of genes upregulated by $BAZ2A_{\Delta TAM}$ and TOP2Ai were also significantly upregulated upon treatment with KDM1Ai and only 2% were downregulated. All these results further support a mechanism by which BAZ2A-TAM domain regulates gene repression in PCa through its interaction with either TOP2A and KDM1A or both (**Fig. 8C**).

Discussion

Previous studies have implicated BAZ2A in aggressive PCa (Gu et al., 2015; Pena-Hernandez et al., 2021; Pietrzak et al., 2020), however, the mechanisms by which BAZ2A regulates gene expression in PCa cells remained elusive. In this work, we showed the importance of BAZ2A-TAM domain and its interaction with RNA in repressing genes critical to PCa.

Studies in mouse non-cancer and differentiated cells showed that BAZ2A-TAM domain associates with the lncRNA pRNA that is required for BAZ2A targeting and silencing of rRNA genes (Anosova et al., 2015; Guetg et al., 2012; Leone et al., 2017; Mayer et al., 2006). Here we show that pRNA mediates rRNA gene silencing in PCa cells, but it is not required for the repression of the other BAZ2A-regulated genes. Further, we showed that the TAM domain is not required for BAZ2A binding with BAZ2A-regulated genes whereas it is important for the interaction with rRNA genes (Mayer et al., 2006). These results further support a role of BAZ2A in PCa that goes beyond the known regulation of rRNA gene transcription (Gu et al., 2015; Guetg et al., 2012; Santoro et al., 2002) and suggest different mechanisms by which BAZ2A represses gene expression in PCa cells.

We showed that BAZ2A-TAM domain serves for the association with factors implicated in the regulation of gene expression, chromatin organization, nuclear pore complex, and RNA splicing. Recent work demonstrated that BAZ2A recruitment to target loci, including a class of inactive (C2) enhancers, is mainly mediated by its bromodomain that specifically interacts with H3K14ac (Peña-Hernández et al., 2021). Our results indicate that BAZ2A regulation in PCa cells depends on both the bromo and the TAM domains; the bromodomain acts as an epigenetic reader targeting BAZ2A to chromatin regions enriched in H3K14ac whereas the TAM domain serves for the association with factors that impact gene expression (**Fig. 8C**).

We showed that BAZ2A associates with RNA in PCa cells, an interaction that is mediated by the TAM domain. Our data suggested that RNA is required for the interaction of BAZ2A with TOP2A and the histone demethylase KDM1A and our future work will aim to identify these BAZ2A-intercating RNAs. On the other hand, BAZ2A-TAM domain can also mediate protein interactions in a RNA-independent manner as in the case of cohesin components. Interestingly, the interaction of KDM1A with RNA has been previously reported by showing that the long intergenic noncoding RNAs (lincRNAs) HOTAIR serves as a scaffold that mediates the

interaction of KDM1A and PRC2, thereby coordinating targeting of histone H3K27me3 and H3K4 demethylation on target genes (Tsai et al., 2010). Thus, by analogy, BAZ2A might recruit KDM1A to target sites through a yet unknown RNA. The reported ability of KDM1A to demethylate mono- and di-methylated lysine 4 of histone H3 (Rudolph et al., 2013) can probably serve to keep BAZ2A-bound C2-enhancers in an inactive state and thus contributing to gene repression. Accordingly, treatment of PC3 cells with KDM1A inhibitors upregulated the expression of genes repressed by BAZ2A-TAM domain and located close to inactive BAZ2A-bound C2-enhancers that are characterized by low H3K4me1 and H3K27ac levels (Peña-Hernández et al., 2021). Moreover, our results showed that BAZ2A-TAM repressed genes are frequently repressed in both primary and metastatic PCas with elevated expression of both BAZ2A and KDM1A or TOP2A. KDM1A is highly expressed in various human malignancies and its activities were linked to carcinogenesis, making it a possible target for anticancer treatments (Maiques-Diaz and Somervaille, 2016). In particular, KDM1A was shown to promote the survival of CRPC by activating the lethal PCa gene network and supporting the proliferation of PCa cells (Liang et al., 2017; Sehrawat et al., 2018). Further, several inhibitors were recently shown to reduce the proliferative potential of PCa cells and prostate cancer growth (Etani et al., 2019; Yang et al., 2017). Thus, the association of KDM1A with BAZ2A defined novel mechanisms by which KDM1A can act in PCa.

The other BAZ2A-TAM domain and RNA dependent associating factor is TOP2A. As in the case of KDM2A, also TOP2A has been reported to be frequently overexpressed in aggressive PCa and serves as an indicator of a poor outcome (Cheville et al., 2008; de Resende et al., 2013; Labbé et al., 2017). Further, high levels of TOP2A were also found in CRPC (Hughes et al., 2006). Despite these correlations, however, the exact mechanism underlying the more aggressive phenotype associated with TOP2A is not known. Interestingly, BAZ2A-TOP2A interaction was previously detected in mouse embryonic stem cells (ESCs), where BAZ2A does not associate with rRNA genes and rRNA gene silencing is impaired (Dalcher et al., 2020). As in the case of PCa cells, BAZ2A and TOP2A in ESCs were shown to act together for the regulation of gene expression, suggesting that BAZ2A-TOP2A crosstalk is conserved among different species and cell context. In PCa, it has been reported that TOP2A cooperates with androgen receptor (AR) to induce transcription of target genes, suggesting that androgen

ablation therapy might be less effective in the presence of high level of TOP2A protein (Schaefer-Klein et al., 2015). In the case of BAZ2A, however, TOP2A activity seems to be related to gene repression, suggesting the TOP2A can act as activator or repressor depending on its interacting partners. The requirement of RNA for the association of TOP2A with BAZ2A suggests that TOP2A might be an RNA-binding protein. Consistent with this, recent high-resolution mapping of RNA-binding proteins detected a significant interaction of TOP2A with RNA (He et al., 2016; Mullari et al., 2017; Perez-Perri et al., 2018). However, it remains to be investigated whether RNA in general or a specific RNA can mediate the association of TOP2A with distinct complexes, thereby specifying activating and/or repressing roles in gene expression. Finally, our data also revealed that tumours expressing high BAZ2A levels also express high levels of KDM1A and TOP2A, suggesting common regulatory pathways. Indeed, a large portion of genes repressed through BAZ2A-TAM domain could also be derepressed by pharmacological inhibition of both KDM1A and TOP2A, indicating that in some cases TOP2A and KDM1A can act together in gene repression, although we cannot exclude cases where they act separately together with BAZ2A. In conclusion, our findings indicate that RNA-mediated interactions between BAZ2A and TOP2A and KDM1A are implicated in PCa and may prove to be useful for the stratification of prostate cancer risk and treatment in patients.

Funding

This work was supported by the Swiss National Science Foundation (31003A_173056 and 201268 to RS), the National Center of Competence in Research RNA & Disease (funded by the SNSF), Forschungskredit of the University of Zurich (to M.R.), Olga Mayenfisch Stifung, Krebsliga Zurich, Swiss Cancer Research Foundation (KFS-4527-08-2018-R; KFS-5488-02-2022), and ERC grant (ERC-AdG-787074-NucleolusChromatin).

Acknowledgement

We thank Rostyslav Kuzyakiv for help in bioinformatic analyses. We thank Peter Hunziker, Catherine Aquino, and the Functional Genomic Center Zurich for the assistance in sequencing and proteomic analysis.

Conflict of interest

The authors declare they have no conflict of interest.

Materials and Methods

Culture of PC3 cells

The PC3 cell line was purchased from the American Type Culture Collection. PC3 cells were cultured in RPMI 1640 medium and Ham's F12 medium (1:1; Gibco) containing 10% FBS (Gibco) and 1% penicillin-streptomycin (Gibco). $2.5x10^6$ cells were seeded in 150 mm tissue culture dishes (TPP®) and cultured for 2 to 3 days. All cells were regularly tested for mycoplasma contamination. The F/H-BAZ2A PC3 cell line was described in (Peña-Hernández et al., 2021).

Construct design

cDNA corresponding to HA-FLAG tagged mouse wild type BAZ2A (H/F-$BAZ2A_{WT}$), CopGFP and shBAZ2A for human BAZ2A were cloned into DC-DON-SH01 vector (GeneCopoeia). Site-directed mutagenesis was performed to create BAZ2A mutants WY531/532GA (H/F-$BAZ2A_{WY/GA}$) and ΔTAM (HA/FLAG-$BAZ2A_{\Delta TAM}$). The sequencing of plasmids was performed to ensure fidelity of sequences.

Plasmid transfections

$1x10^6$ of PC3 cells were seeded in 100 mm culture dish (TPP®), grown for 24 hours and transfected with 8 µg of plasmids and 8 µl of X-tremeGENE HP DNA Transfection Reagent (Roche). The cells were grown for 48 hours post-transfection and collected for downstream analyses.

RNA purification, reverse transcription, and quantitative PCR

RNA was purified with TRIzol reagent (Life Technologies). 1µg total RNA was primed with random hexamers and reverse-transcribed into cDNA using MultiScribe™ Reverse Transcriptase (Life Technologies). Amplification of samples without reverse transcriptase assured absence of genomic or plasmid DNA (data not shown). The relative transcription levels were determined by normalization to *GAPDH or β-actin* mRNA levels, as indicated. qRT-PCR was performed with KAPA SYBR® FAST (Sigma) on Rotor-Gene RG-3000 A (Corbett Research).

Treatment of PC3 cells with ICRF-193 and LG-001

$1x10^6$ PC3 cells were seeded in 100 mm culture dish (TPP®), 24 hours prior to the treatment. ICRF-193 (Sigma) or OG-L002 (MedChemExpress) were added directly to the medium to a final 10 µM concentration. Cells were harvested for downstream analyses 48 hours after treatment with the inhibitors.

Chromatin immunoprecipitation

ChIP experiments were performed as previously described (Leone et al., 2017; Peña-Hernández et al., 2021). Briefly, 1% formaldehyde was added to cultured cells to cross-link proteins to DNA. Isolated nuclei were then digested with MNase (S7 Micrococcal nuclease, Roche) and briefly sonicated using a Bioruptor ultrasonic cell disruptor (Diagenode) to shear genomic DNA to an average fragment size of 200 bp. 200 µg of chromatin was diluted tenfold with ChIP buffer (16.7 mM Tris-HCl pH 8.1, 167 mM NaCl, 1.2 mM EDTA, 0.01% SDS and 1.1% Triton X-100) and precleared for 2h with 10 µl of packed Sepharose beads for at least 2h at 4°C. Immunoprecipitation was performed overnight with the HA-magnetic beads (Pierce™ Anti-HA magnetic beads, ThermoFisher Scientific). After washing, elution and reversion of cross-links, eluates were treated with RNase A (1µg). DNA was purified with phenol-chloroform, ethanol precipitated and quantified by quantitative PCR.

RNAseq and data analysis

$1.5x10^5$ PC3 cells were seeded into each well of a 6-well culture dish (TPP®), grown for 24 hours, and transfected with constructs expressing either H/F-BAZ2A$_{WT}$ or H/F-BAZ2A$_{\Delta TAM}$ with simultaneous downregulation of endogenous human BAZ2A. 4 µg of plasmid and 4 µl of X-tremeGENE HP DNA Transfection Reagent (Roche) were used per well. The cells were grown for 48 hours post-transfection, collected by trypsinization, and pooled. Using fluorescence activated cells sorting (FACS), the GFP(+) cells expressing H/F-BAZ2A$_{WT}$ or H/F-BAZ2A$_{\Delta TAM}$ were collected and their total RNA purified with TRIzol reagent (Life Technologies) as described above. Total RNA from 3 independent samples from PC3 cells expressing H/F-BAZ2A$_{WT}$ and from three independent samples expressing H/F-BAZ2A$_{\Delta TAM}$ were obtained. DNA contaminants

were removed by treating RNA with 2U TURBO DNase I (Invitrogen) for 1h at 37°C and the RNA samples were re-purified using TRIzol. The quality of the isolated RNA was determined by Bioanalyzer 2100 (Agilent, Waldbronn, Germany). Only those samples with a 260nm/280nm ratio between 1.8–2.1 and a 28S/18S ratio within 1.5–2 were further processed. The TruSeq RNA Sample Prep Kit v2 (Illumina, Inc, California, USA) was used in the succeeding steps. Briefly, total RNA samples (100-1000ng) were poly(A) enriched and then reverse-transcribed into double-stranded cDNA. The cDNA samples were fragmented, end-repaired and polyadenylated before ligation of TruSeq adapters containing the index for multiplexing. Fragments containing TruSeq adapters on both ends were selectively enriched with PCR. The quality and quantity of the enriched libraries were validated using Qubit® (1.0) Fluorometer and the Caliper GX LabChip® GX (Caliper Life Sciences, Inc., USA). The product was a smear with an average fragment size of approximately 260bp. The libraries were normalized to 10nM in Tris-Cl 10mM, pH8.5 with 0.1% Tween 20. The TruSeq SR Cluster Kit HS4000 (Illumina, Inc, California, USA) was used for cluster generation using 10pM of pooled normalized libraries on the cBOT. Sequencing was performed on the Illumina HiSeq 2500 single end 100bp using the TruSeq SBS Kit HS2500 (Illumina, Inc, California, USA). Reads were aligned to the reference genome (hg38) with Subread (i.e. subjunc, version 1.4.6-p4; (Liao et al., 2013)) allowing up to 16 alignments per read (options: –trim5 10 –trim3 15 -n 20 - m 5 -B 16 -H –allJunctions). Count tables were generated with Rcount (Schmid and Grossniklaus, 2015) and with an allocation distance of 10bp for calculating the weights of the reads with multiple alignments, considering the strand information, and a minimal number of 5 hits. Variation in gene expression was analyzed with a general linear model in R with the package edgeR (version 3.12.0; (Robinson and Oshlack, 2010)). Genes differentially expressed between specific conditions were identified with linear contrasts using trended dispersion estimates and Benjamini-Hochberg multiple testing corrections. Genes with a *P*-value below 0.05 and a minimal fold change of 1.5 were considered as differentially expressed. These thresholds have previously been used characterizing chromatin remodeler functions (de Dieuleveult et al., 2016). Gene ontology analysis was performed with David Bioinformatics Resource 6.8 (Huang da et al., 2009).

BAZ2A co-immunoprecipitation and mass spectrometric analysis

$1x10^6$ PC3 cells were seeded in 100 mm culture dish (TPP®), grown for 24 hrs and transfected with 8 µg of plasmid DNA for expression of HA/FLAG-BAZ2A$_{WT}$, HA/FLAG-BAZ2A$_{WY/GA}$ or HA/FLAG-BAZ2A$_{\Delta TAM}$. Four culture dishes were used per condition. Cells were grown for another 48 hours, harvested by scraping, and washed two times with PBS. Cells were then incubated for 10 min on ice in 3 ml of hypotonic buffer (10 mM HEPES pH 7.6, 1.5 mM $MgCl_2$, 10 mM KCl), spun down for 5 min, at 1000 g at 4°C, supplemented with 0.5% Triton X-100 and incubated for another 10 min at 4°C. Obtained nuclei were spun down for 10 min, at 1000 g at 4°C, resuspended in 500 µl of MNase digestion buffer (0.3 M Sucrose, 50 mM Tris–HCl pH 7.5, 30 mM KCl, 7.5 mM NaCl, 4 mM MgCl2, 1 mM CaCl2, 0.125% NP-40, 0.25% NaDeoxycholate) and supplemented with 50 U of MNase (Roche). Samples were incubated at 30 min at 37°C under shaking. Next the NaCl concentration was brought to 200 mM and samples were incubated for 10 min on ice. Samples were spun down at maximum speed, the pellets discarded, and 10% of the supernatant was collected as input samples. The remaining part of the supernatant was diluted four times with MNase buffer, supplemented with cOmpleteTM Protease Inhibitor Cocktail (Roche) and the samples were incubated overnight at 4°C with orbital shaking with 50 µl of HA magnetic beads (ThermoFisher Scientific) that were pre-washed three times with MNase buffer. The day after, the beads were washed three times for 30 min at 4°C with 1 ml of the wash buffer (20 mM HEPES pH 7.6, 20% glycerol, 200 mM NaCl, 1.5 mM $MgCl_2$, 0.2 mM EDTA, 0.02% NP-40). Half of the beads were further analyzed by Western Blotting whereas the other half was prepared for LC-MS/MS analyses. The dry beads were dissolved in 45 µl buffer containing 10 mM Tris + 2 mM $CaCl_2$, pH 8.2 and 5 µl of trypsin (100 ng/µl in 10 mM HCl) for digestion, which was carried out in a microwave instrument (Discover System, CEM) for 30 min at 5 W and 60°C. Samples were dried in a SpeedVac (Savant), dissolved in 0.1% formic acid (Romil), and an aliquot ranging from 5 to 25% was analyzed on a nanoAcquity UPLC (Waters Inc.) connected to a Q Exactive mass spectrometer (Thermo Scientific) equipped with a Digital PicoView source (NewObjective). Peptides were trapped on a Symmetry C18 trap column (5 µm, 180 µm × 20 mm, Waters Inc.) and separated on a BEH300 C18 column (1.7 µm, 75 µm × 150 m, Waters Inc.) at a flow rate of 250 nl/min using a gradient from 1% solvent B (0.1% formic acid in acetonitrile, Romil)/99% solvent A (0.1% formic acid in

water, Romil) to 40% solvent B/60% solvent A within 90 min. Mass spectrometer settings were as follows: Data-dependent analysis. Precursor scan range 350–1,500 m/z, resolution 70,000, maximum injection time 100 ms, threshold 3e6. Fragment ion scan range 200–2,000 m/z, Resolution 35,000, maximum injection time 120 ms, threshold 1e5. Proteins were identified using the Mascot search engine (Matrix Science, version 2.4.1). Mascot was set up to search the SwissProt database assuming the digestion enzyme trypsin. Mascot was searched with a fragment ion mass tolerance of 0.030 Da and a parent ion tolerance of 10.0 PPM. Oxidation of methionine was specified in Mascot as a variable modification. Scaffold (Proteome Software Inc.) was used to validate MS/MS-based peptide and protein identifications. Peptide identifications were accepted if they achieved a false discovery rate (FDR) of less than 0.1% by the Scaffold Local FDR algorithm. Protein identifications were accepted if they achieved an FDR of less than 1.0% and contained at least two identified peptides.

BAZ2A immunoprecipitation and RNA radiolabelling

$1x10^6$ of PC3 cells and $1x10^6$ H/F-BAZ2A PC3 cells were seeded in 150 mm culture dish (TPP®) and grown for 96 hours. Four dishes were used per condition. For the experiment performed with ectopically expressed H/F-BAZ2A$_{WT}$ and H/F-BAZ2A$_{WY/GA}$, $1x10^6$ PC3 cells were seeded in 100 mm culture dish (TPP®), grown for 24 hours and transfected with 8 µg of plasmid DNA. The proteins were expressed for 48 hours. Fifteen 100 mm dishes were used per condition.

Cells were washed with 5 ml of cold PBS, 2 ml of fresh and cold PBS was added and the cells were UV-B cross-linked with 400 mJ in UV-irradiator (Vilber). Cells were harvested by scraping, spun down at 1000 g for 5 min at 4°C, resuspended in 3 ml of the hypotonic buffer (10 mM HEPES pH 7.6, 1.5 mM $MgCl_2$, 10 mM KCl), and incubated for 15 min on ice. Next, cells were supplemented with 0.5% Triton X-100 and cOmpleteTM Protease Inhibitor Cocktail (Roche), incubated on ice for another 15 min and spun down at 1000 g for 5 min at 4°C. The pellet was resuspended in 500 µl of lysis buffer (50 mM TRIS-HCl pH 7.4, 100 mM NaCl, 0.1% SDS, 1% NP-40, 0.5% NaDeoxycholate) supplemented with cOmpleteTM Protease Inhibitor Cocktail (Roche) and incubated on ice for 10 min. 2 U of DNase (TURBO™ DNase, ThermoFisher Scientific) and 0.02 U (high RNase treatment) or 0.0025 U (low RNase treatment) of RNase I (Ambion) was added to the lysates. Lysates were incubated at 37°C with shaking for exactly 2

min and immediately supplemented with 40 U of RNase inhibitor (RiboLock RNase Inhibitor, ThermoFisher Scientific) followed by 3 min incubation on ice. The NaCl concentration was brought to 400 mM followed by 10 min incubation at 4°C with orbital shaking. Samples were spun down at maximal speed for 5 min at 4°C and supplemented with 800 µl of no-salt lysis buffer (50 mM Tris-HCl pH 7.4, 0.1% SDS, 1% NP-40, 0.5% NaDeoxycholate), 40 U of RNase inhibitor and with cOmplete TM Protease Inhibitor Cocktail (Roche). For the input for Western blot analysis, 8% of each sample was taken and stored at -20°C. Samples were incubated overnight at 4°C with orbital shaking with 50 µl of HA magnetic beads (Pierce™ Anti-HA magnetic beads, ThermoFisher Scientific) pre-washed with no-salt lysis buffer. Beads were washed twice for 30 min at 4°C with 1 ml of high-salt wash buffer (50 mM Tris-HCl pH 7.4, 1 M NaCl, 1 mM EDTA, 1% NP-40, 0.1% SDS, 0.5% NaDeoxycholate) and once with low-salt wash buffer (20 mM Tris-HCl pH 7.4, 10 mM $MgCl_2$, 0.2% Tween-20). 10% of the beads were taken for Western blot analyses. The remaining beads were resuspended in 20 µl of the radiolabelling mixture (10U of T4 polynucleotides Kinase (Thermo Scientific), reaction buffer A (Thermo Scientific) and 5 µCi of [gamma-P^{32}]ATP (Hartmann Analytic)) and incubated for 10 min at 37°C with shaking. The supernatants were removed and the beads washed with 300 µl of low-salt lysis buffer. Samples were supplemented with 37 nM DTT and NuPAGE loading dye and incubated at 70°C for 10 min with shaking. Samples were spun down for 1 min at RT at max speed, the supernatants were loaded on 3-8% NuPAGE TRIS-Acetate gels (ThermoFisher Scientific) and run for 90 min at 150 V. The gels were transferred to the nitrocellulose membrane with iBLOT 2 Dry Blotting System (Invitrogen). The membrane containing radioactive samples was covered with light-sensitive film (Typox™) and exposed in darkness for 16 hours at -80°C.

BAZ2A co-immunoprecipitation with RNase A treatment

$2x10^6$ of PC3 WT cells and $1x10^6$ H/F-BAZ2A PC3 cells were seeded in 150 mm culture dish (TPP®) and grown for 48 hrs. Five culture dishes were used per condition. Cells were harvested by scraping and washed two times with PBS. Cells were incubated for 10 min on ice in 4 ml of hypotonic buffer (10 mM HEPES pH 7.6, 1.5 mM $MgCl_2$, 10 mM KCl), spun down for 5 min, at 1000 xg at 4°C, supplemented with 0.5% Triton X-100, and incubated for another 10 min at 4°C. Obtained nuclei were spun down for 10 min, at 1000 g at 4°C, resuspended in 500 µl of

MNase digestion buffer (0.3 M Sucrose, 50 mM Tris–HCl pH 7.5, 30 mM KCl, 7.5 mM NaCl, 4 mM MgCl2, 1 mM CaCl2, 0.125% NP-40, 0.25% NaDeoxycholate) and supplemented with 40 U of MNase (Roche). Samples were shacked for 30 min at 37°C. Next, the NaCl concentration was brought to 200 mM and samples were incubated for 10 min on ice. Samples were spun down at maximum speed. The pellets were discarded and 10% of the supernatant was collected as an input and further analysed by Western blot. The remaining part of the supernatant was diluted four times with MNase buffer, supplemented with cOmpleteTM Protease Inhibitor Cocktail (Roche) and 100 µg/ml RNase A (ThermoFisher). The control samples were not treated with RNase A. The samples were incubated overnight at 4°C with orbital shaking with 25 µl of HA magnetic beads (Pierce™ Anti-HA magnetic beads, ThermoFisher Scientific) pre-washed three times with MNase buffer. The beads were washed three times for 30 min at 4°C with 1 ml of the wash buffer (20 mM HEPES ph 7.6, 20% glycerol, 200 mM NaCl, 1.5 mM $MgCl_2$, 0.2 mM EDTA, 0.02% NP-40) resuspended in a small volume of wash buffer. All the samples were loaded on a 6% home-made SDS-PAGE gel, run for 130 min at 120 V and analysed further by Western blot.

References

Anosova, I., Melnik, S., Tripsianes, K., Kateb, F., Grummt, I., and Sattler, M. (2015). A novel RNA binding surface of the TAM domain of TIP5/BAZ2A mediates epigenetic regulation of rRNA genes. Nucleic Acids Res *43*, 5208-5220.

Cancer Genome Atlas Research, N. (2015). The Molecular Taxonomy of Primary Prostate Cancer. Cell *163*, 1011-1025.

Chandran, U.R., Ma, C., Dhir, R., Bisceglia, M., Lyons-Weiler, M., Liang, W., Michalopoulos, G., Becich, M., and Monzon, F.A. (2007). Gene expression profiles of prostate cancer reveal involvement of multiple molecular pathways in the metastatic process. BMC Cancer *7*, 64.

Chen, T., Sun, Y., Ji, P., Kopetz, S., and Zhang, W. (2015). Topoisomerase IIalpha in chromosome instability and personalized cancer therapy. Oncogene *34*, 4019-4031.

Cheville, J.C., Karnes, R.J., Therneau, T.M., Kosari, F., Munz, J.M., Tillmans, L., Basal, E., Rangel, L.J., Bergstralh, E., Kovtun, I.V.*, et al.* (2008). Gene panel model predictive of outcome in men at high-risk of systemic progression and death from prostate cancer after radical retropubic prostatectomy. J Clin Oncol *26*, 3930-3936.

Dalcher, D., Tan, J.Y., Bersaglieri, C., Pena-Hernandez, R., Vollenweider, E., Zeyen, S., Schmid, M.W., Bianchi, V., Butz, S., Roganowicz, M.*, et al.* (2020). BAZ2A safeguards genome architecture of ground-state pluripotent stem cells. EMBO J *39*, e105606.

de Dieuleveult, M., Yen, K., Hmitou, I., Depaux, A., Boussouar, F., Bou Dargham, D., Jounier, S., Humbertclaude, H., Ribierre, F., Baulard, C.*, et al.* (2016). Genome-wide nucleosome specificity and function of chromatin remodellers in ES cells. Nature *530*, 113-116.

de Resende, M.F., Vieira, S., Chinen, L.T., Chiappelli, F., da Fonseca, F.P., Guimarães, G.C., Soares, F.A., Neves, I., Pagotty, S., Pellionisz, P.A.*, et al.* (2013). Prognostication of prostate cancer based on TOP2A protein and gene assessment: TOP2A in prostate cancer. J Transl Med *11*, 36.

Etani, T., Naiki, T., Naiki-Ito, A., Suzuki, T., Iida, K., Nozaki, S., Kato, H., Nagayasu, Y., Suzuki, S., Kawai, N.*, et al.* (2019). NCL1, A Highly Selective Lysine-Specific Demethylase 1 Inhibitor, Suppresses Castration-Resistant Prostate Cancer Growth via Regulation of Apoptosis and Autophagy. J Clin Med *8*.

Gu, L., Frommel, S.C., Oakes, C.C., Simon, R., Grupp, K., Gerig, C.Y., Bar, D., Robinson, M.D., Baer, C., Weiss, M.*, et al.* (2015). BAZ2A (TIP5) is involved in epigenetic alterations in prostate cancer and its overexpression predicts disease recurrence. Nat Genet *47*, 22-30.

Guetg, C., Lienemann, P., Sirri, V., Grummt, I., Hernandez-Verdun, D., Hottiger, M.O., Fussenegger, M., and Santoro, R. (2010). The NoRC complex mediates the heterochromatin formation and stability of silent rRNA genes and centromeric repeats. EMBO J *29*, 2135-2146.

Guetg, C., Scheifele, F., Rosenthal, F., Hottiger, M.O., and Santoro, R. (2012). Inheritance of Silent rDNA Chromatin Is Mediated by PARP1 via Noncoding RNA. Mol Cell *45*, 790-800.

Hanahan, D., and Weinberg, R.A. (2011). Hallmarks of cancer: the next generation. Cell *144*, 646-674.

He, C., Sidoli, S., Warneford-Thomson, R., Tatomer, D.C., Wilusz, J.E., Garcia, B.A., and Bonasio, R. (2016). High-Resolution Mapping of RNA-Binding Regions in the Nuclear Proteome of Embryonic Stem Cells. Mol Cell *64*, 416-430.

Huang da, W., Sherman, B.T., and Lempicki, R.A. (2009). Systematic and integrative analysis of large gene lists using DAVID bioinformatics resources. Nature protocols *4*, 44-57.

Hughes, C., Murphy, A., Martin, C., Fox, E., Ring, M., Sheils, O., Loftus, B., and O'Leary, J. (2006). Topoisomerase II-alpha expression increases with increasing Gleason score and with hormone insensitivity in prostate carcinoma. Journal of clinical pathology *59*, 721-724.

Ishida, R., Miki, T., Narita, T., Yui, R., Sato, M., Utsumi, K.R., Tanabe, K., and Andoh, T. (1991). Inhibition of intracellular topoisomerase II by antitumor bis(2,6-dioxopiperazine) derivatives: mode of cell growth inhibition distinct from that of cleavable complex-forming type inhibitors. Cancer Res *51*, 4909-4916.

Kahl, P., Gullotti, L., Heukamp, L.C., Wolf, S., Friedrichs, N., Vorreuther, R., Solleder, G., Bastian, P.J., Ellinger, J., Metzger, E.*, et al.* (2006). Androgen receptor coactivators lysine-specific histone demethylase 1 and four and a half LIM domain protein 2 predict risk of prostate cancer recurrence. Cancer research *66*, 11341-11347.

Kashyap, V., Ahmad, S., Nilsson, E.M., Helczynski, L., Kenna, S., Persson, J.L., Gudas, L.J., and Mongan, N.P. (2013). The lysine specific demethylase-1 (LSD1/KDM1A) regulates VEGF-A expression in prostate cancer. Mol Oncol *7*, 555-566.

Labbé, D.P., Sweeney, C.J., Brown, M., Galbo, P., Rosario, S., Wadosky, K.M., Ku, S.-Y., Sjöström, M., Alshalalfa, M., Erho, N.*, et al.* (2017). TOP2A and EZH2 Provide Early Detection of an Aggressive Prostate Cancer Subgroup. Clinical Cancer Research *23*, 7072-7083.

Lee, F.C.Y., and Ule, J. (2018). Advances in CLIP Technologies for Studies of Protein-RNA Interactions. Mol Cell *69*, 354-369.

Leone, S., Bar, D., Slabber, C.F., Dalcher, D., and Santoro, R. (2017). The RNA helicase DHX9 establishes nucleolar heterochromatin, and this activity is required for embryonic stem cell differentiation. EMBO Rep *18*, 1248-1262.

Li, C., Wu, W., Ding, H., Li, Q., and Xie, K. (2018). The transcription factor 7 like 2-binding protein TIP5 activates beta-catenin/transcription factor signaling in hepatocellular carcinoma. Mol Med Rep *17*, 7645-7651.

Li, J.J., and Shen, M.M. (2018). Prostate Stem Cells and Cancer Stem Cells. Cold Spring Harbor Perspectives in Medicine.

Liang, Y., Ahmed, M., Guo, H., Soares, F., Hua, J.T., Gao, S., Lu, C., Poon, C., Han, W., Langstein, J.*, et al.* (2017). LSD1-Mediated Epigenetic Reprogramming Drives CENPE Expression and Prostate Cancer Progression. Cancer research *77*, 5479-5490.

Liao, Y., Smyth, G.K., and Shi, W. (2013). The Subread aligner: fast, accurate and scalable read mapping by seed-and-vote. Nucleic Acids Res *41*, e108.

Maiques-Diaz, A., and Somervaille, T.C. (2016). LSD1: biologic roles and therapeutic targeting. Epigenomics *8*, 1103-1116.

Mayer, C., Schmitz, K.M., Li, J., Grummt, I., and Santoro, R. (2006). Intergenic transcripts regulate the epigenetic state of rRNA genes. Mol Cell *22*, 351-361.

Mullari, M., Lyon, D., Jensen, L.J., and Nielsen, M.L. (2017). Specifying RNA-Binding Regions in Proteins by Peptide Cross-Linking and Affinity Purification. J Proteome Res *16*, 2762-2772.

Pena-Hernandez, R., Aprigliano, R., Carina Frommel, S., Pietrzak, K., Steiger, S., Roganowicz, M., Lerra, L., Bizzarro, J., and Santoro, R. (2021). BAZ2A-mediated repression via H3K14ac-marked enhancers promotes prostate cancer stem cells. EMBO Rep, e53014.

Peña-Hernández, R., Aprigliano, R., Frommel, S., Pietrzak, K., Steiger, S., Roganowicz, M., Lerra, L., Bizzarro, J., and Santoro, R. (2021). BAZ2A-mediated repression via H3K14ac-marked enhancers promotes prostate cancer stem cells. EMBO Rep *in press*, bioRxiv, 2020.2007.2003.185843.

Perez-Perri, J.I., Rogell, B., Schwarzl, T., Stein, F., Zhou, Y., Rettel, M., Brosig, A., and Hentze, M.W. (2018). Discovery of RNA-binding proteins and characterization of their dynamic responses by enhanced RNA interactome capture. Nat Commun *9*, 4408.

Pietrzak, K., Kuzyakiv, R., Simon, R., Bolis, M., Bar, D., Aprigliano, R., Theurillat, J.P., Sauter, G., and Santoro, R. (2020). TIP5 primes prostate luminal cells for the oncogenic transformation mediated by PTEN-loss. Proc Natl Acad Sci U S A *117*, 3637-3647.

Robinson, D., Van Allen, E.M., Wu, Y.M., Schultz, N., Lonigro, R.J., Mosquera, J.M., Montgomery, B., Taplin, M.E., Pritchard, C.C., Attard, G.*, et al.* (2015). Integrative clinical genomics of advanced prostate cancer. Cell *161*, 1215-1228.

Robinson, M.D., and Oshlack, A. (2010). A scaling normalization method for differential expression analysis of RNA-seq data. Genome Biol *11*, R25.

Rudolph, T., Beuch, S., and Reuter, G. (2013). Lysine-specific histone demethylase LSD1 and the dynamic control of chromatin. Biological chemistry *394*, 1019-1028.

Santoro, R., Li, J., and Grummt, I. (2002). The nucleolar remodeling complex NoRC mediates heterochromatin formation and silencing of ribosomal gene transcription. Nat Genet *32*, 393-396.

Savic, N., Bar, D., Leone, S., Frommel, S.C., Weber, F.A., Vollenweider, E., Ferrari, E., Ziegler, U., Kaech, A., Shakhova, O.*, et al.* (2014). lncRNA Maturation to Initiate Heterochromatin Formation in the Nucleolus Is Required for Exit from Pluripotency in ESCs. Cell Stem Cell *15*, 720-734.

Schaefer-Klein, J.L., Murphy, S.J., Johnson, S.H., Vasmatzis, G., and Kovtun, I.V. (2015). Topoisomerase 2 Alpha Cooperates with Androgen Receptor to Contribute to Prostate Cancer Progression. PLoS One *10*, e0142327.

Schmid, M.W., and Grossniklaus, U. (2015). Rcount: simple and flexible RNA-Seq read counting. Bioinformatics *31*, 436-437.

Sehrawat, A., Gao, L., Wang, Y., Bankhead, A., 3rd, McWeeney, S.K., King, C.J., Schwartzman, J., Urrutia, J., Bisson, W.H., Coleman, D.J.*, et al.* (2018). LSD1 activates a lethal prostate cancer gene network independently of its demethylase function. Proceedings of the National Academy of Sciences of the United States of America *115*, E4179-e4188.

Siegel, R.L., Miller, K.D., and Jemal, A. (2015). Cancer statistics, 2015. CA: a cancer journal for clinicians *65*, 5-29.

Strohner, R., Nemeth, A., Jansa, P., Hofmann-Rohrer, U., Santoro, R., Langst, G., and Grummt, I. (2001). NoRC--a novel member of mammalian ISWI-containing chromatin remodeling machines. EMBO J *20*, 4892-4900.

Sung, H., Ferlay, J., Siegel, R.L., Laversanne, M., Soerjomataram, I., Jemal, A., and Bray, F. (2021). Global cancer statistics 2020: GLOBOCAN estimates of incidence and mortality worldwide for 36 cancers in 185 countries. CA Cancer J Clin.

Szklarczyk, D., Franceschini, A., Wyder, S., Forslund, K., Heller, D., Huerta-Cepas, J., Simonovic, M., Roth, A., Santos, A., Tsafou, K.P.*, et al.* (2015). STRING v10: protein-protein interaction networks, integrated over the tree of life. Nucleic Acids Res *43*, D447-452.

Tsai, M.C., Manor, O., Wan, Y., Mosammaparast, N., Wang, J.K., Lan, F., Shi, Y., Segal, E., and Chang, H.Y. (2010). Long noncoding RNA as modular scaffold of histone modification complexes. Science *329*, 689-693.

Varambally, S., Yu, J., Laxman, B., Rhodes, D.R., Mehra, R., Tomlins, S.A., Shah, R.B., Chandran, U., Monzon, F.A., Becich, M.J.*, et al.* (2005). Integrative genomic and proteomic analysis of prostate cancer reveals signatures of metastatic progression. Cancer Cell *8*, 393-406.

Yadav, S.S., Stockert, J.A., Hackert, V., Yadav, K.K., and Tewari, A.K. (2018). Intratumor heterogeneity in prostate cancer. Urologic Oncology: Seminars and Original Investigations *36*, 349-360.

Yang, C., Wang, W., Liang, J.-X., Li, G., Vellaisamy, K., Wong, C.-Y., Ma, D.-L., and Leung, C.-H. (2017). A Rhodium(III)-Based Inhibitor of Lysine-Specific Histone Demethylase 1 as an Epigenetic Modulator in Prostate Cancer Cells. Journal of Medicinal Chemistry *60*, 2597-2603.

Yu, Y.P., Landsittel, D., Jing, L., Nelson, J., Ren, B., Liu, L., McDonald, C., Thomas, R., Dhir, R., Finkelstein, S.*, et al.* (2004). Gene expression alterations in prostate cancer predicting tumor aggression and preceding development of malignancy. Journal of clinical oncology : official journal of the American Society of Clinical Oncology *22*, 2790-2799.

Zhong, Z., Yu, J., Virshup, D.M., and Madan, B. (2020). Wnts and the hallmarks of cancer. Cancer metastasis reviews *39*, 625-645.

Figure legends

Figure 1

The TAM domain is required for BAZ2A binding to the RNA in PCa cells

A. BAZ2A interacts with RNA in PC3 cells. Top panel. Western blot showing anti-HA immunoprecipitates from H/F-BAZ2A$_{end}$ PC3 cells and parental PC3 cells crosslinked with UV-light and treated with low (0.0025U) or high (0.02U) amount of RNase I. BAZ2A signal was detected with anti-HA antibodies. Bottom panel. Autoradiography showing ^{32}P-radiolabeled-RNA from the indicated anti-HA immunoprecipitates.

B. BAZ2A interaction with RNA depend on TAM domain. Top panel. Western blot showing anti-HA immunoprecipitates from PC3 cells transfected with plasmids expressing H/F-BAZ2A$_{WT}$ and H/F-BAZ2A$_{WY/GA}$ that were UV-light irradiated and treated with 0.0025U RNase I. BAZ2A signal was detected with anti-BAZ2A antibodies. Bottom panel. Autoradiography showing ^{32}P-radiolabeled-RNA from the indicated anti-HA immunoprecipitates.

C. A scheme of the strategy used to measure gene expression in PC3 cells overexpressing the lncRNA pRNA. rDNA$_{pr}$ represents the promoter of human rRNA genes. GFP expression was under the control of EF1α promoter.

D. qRT-PCR of GFP(+)-FACS-sorted PC3 cells showing pRNA, 45S pre-rRNA and mRNA levels of known and validated BAZ2A target genes that are repressed by BAZ2A (Gu et al., 2015). Transcript levels were normalized to *GAPDH* and cells transfected with RNA-control. Error bars represent standard deviation of three independent experiments. Statistical significance (*P*-value) was calculated using two-tailed t-test (**<0.01, ***< 0.001); ns: not significant.

Figure 2

BAZ2A regulates a set of genes involved in PCa development through its RNA-binding TAM domain

A. A scheme of the all-in-one plasmids for the expression of mouse HA-FLAG BAZ2A (H/F-mBAZ2A) under CMV promoter, GFP reporter gene under EF1α promoter and shRNA for endogenous human (h)BAZ2A under H1 promoter.

B. Western blot of GFP(+)-FACS-sorted PC3 cells transfected with all-in-one plasmids expressing H/F-mBAZ2A$_{WT}$ and H/F-mBAZ2A$_{\Delta TAM}$. BAZ2A signal was detected with anti-HA antibodies. Nucleolin served as a loading control.

C. GFP(+)-FACS-sorted PC3 cells transfected with all-in-one constructs expressing H/F-mBAZ2A$_{WT}$ and H/F-mBAZ2A$_{\Delta TAM}$ with simultaneous downregulation of endogenous human BAZ2A. qRT-PCR showing mRNA levels of human BAZ2A (left) and total (human and mouse) BAZ2A (right). Control cells were transfected with plasmids only expressing GFP. mRNA levels were normalized to *GAPDH*. Error bars represent standard deviation of three independent experiments. Statistical significance (*P*-value) was calculated using paired two-tailed t-test (***< 0.001, ****<0.0001).

D. BAZ2A regulates gene expression in PC3 cells. MA plot of the $\log_2$ fold change (FC) gene expression of GFP(+)-FACS-sorted PC3 cells expressing BAZ2A$_{\Delta TAM}$ compared cells expressing BAZ2A$_{WT}$. Gene expression values of three replicates were averaged. Blue points represent upregulated genes ($\log_2$FC > 0.58) and red points show downregulated genes ($\log_2$FC < -0.58) and *P* value < 0.05.

E. Top eleven gene ontology (GO) terms as determined using DAVID for genes upregulated and downregulated in PC3 cells expressing BAZ2A$_{\Delta TAM}$ compared to cells expressing BAZ2A$_{WT}$.

F. Pie chart showing the number of genes significantly affected by BAZ2A$_{\Delta TAM}$ expression that are upregulated (upper panel) or downregulated (bottom panel) in PC3 cells upon Baz2A knockdown (Pena-Hernandez et al., 2021). On the right, it is shown the number of genes upregulated and downregulated upon BAZ2A$_{\Delta TAM}$ expression.

G. BAZ2A regulates the expression of genes frequently repressed in metastatic mPCa through its TAM domain. qRT-PCR showing mRNA levels of the genes frequently repressed in mPCa upon expression of BAZ2A$_{WT}$ and BAZ2A$_{\Delta TAM}$ domain in GFP(+)-FACS-sorted PC3 cells. Control cells were transfected with plasmids only expressing GFP. mRNA levels were normalized to *GAPDH* mRNA and control cells transfected with plasmid expressing GFP. Error bars represent standard deviation of three independent experiments. Statistical significance (*P*-value) was calculated using two-tailed t-test (*<0.05, **<0.01, ***< 0.001, ****<0.0001).

Figure 3

BAZ2A-TAM domain is required for the repression of a set of genes that have their enhancers bound by BAZ2A

A. A schema showing BAZ2A-BRD-mediated association with C2-enhancer enriched in H3K14ac and the linearly nearest gene in PC3 cells.

B. Levels of BAZ2A and the histone modifications H3K14ac, H3K27me3, and H3K27ac at active C1-enhancers (i.e. active enhancers marked by H3K27ac, H3K4me1, and DNase I hypersensitive sites) and inactive C2-enhancer bound or not bound by BAZ2A (Peña-Hernández et al., 2021). Read coverage was measured at ±1Kb from annotated enhancer regions. Values are shown as average RPKM. Statistical significance (P-values) was calculated using the unpaired two-tailed t test (*<0.05, ****<0.0001).

C. Right panel. Pie charts showing the number of genes in the nearest linear genome proximity to BAZ2A-bound C2-enhancers and their significant expression changes in PC3 cells expressing $BAZ2A_{\Delta TAM}$ compared to PC3 cells expressing $BAZ2A_{WT}$. Genes significantly affected by $BAZ2A_{\Delta TAM}$ expression: $\log_2$ fold change ±0.1, $P < 0.05$.

D. Wiggle tracks showing RNA levels in PC3 cells expressing $BAZ2A_{WT}$ and $BAZ2A_{\Delta TAM}$, occupancy of BAZ2A, C2 enhancer, and its nearest gene *CSF2*.

E. Top 10 gene ontology (GO) terms of genes in the nearest linear genome proximity to BAZ2A-bound C2-enhancers and significantly upregulated in PC3 cells expressing $BAZ2A_{\Delta TAM}$.

F. BAZ2A-TAM domain is not implicate in BAZ2A association with C2-enhancers. HA-ChIP analysis of PC3 cells transfected with vectors expressing only GFP (-), H/F- $BAZ2A_{WT}$, and H/F-$BAZ2A_{\Delta TAM}$ showing the association of BAZ2A with the nearest C2-enhancers (enh.) to genes derepressed by $BAZ2A_{\Delta TAM.}$ The association with the promoter of BAZ2A-regulated gene *AOX1* and rRNA genes is also shown. Values were normalized to the corresponding inputs and control samples (-). Values are from two independent experiments. Grey and black dots represent the values obtained from each single experiment.

Figure 4

BAZ2A associates with TOP2A and KDM1A through TAM domain and RNA in PCa cells

A. HA-BAZ2A immunoprecipitation from nuclear extracts of PC3 cells transfected with plasmids expressing H/F-BAZ2A$_{WT}$ and H/F-BAZ2A$_{WY/GA}$. BAZ2A signal was detected with anti-HA antibodies. The interaction with SNF2H was visualized with anti-SNF2H antibodies.

B. Mass spectrometry analysis of H/F-BAZ2A$_{WT}$ and H/F-BAZ2A$_{WY/GA}$ immunoprecipitates from PC3 cells. Values represent average of peptide numbers from three independent experiments. Values in orange represent proteins with decreased association with BAZ2A$_{WY/GA}$ compared to BAZ2A$_{WT}$.

C. STRING analysis depicting functional protein association networks of BAZ2A-interacting proteins that depend on a functional TAM domain.

D. HA-BAZ2A immunoprecipitation of nuclear extracts for PC3 cells transfected with plasmids expressing H/F-BAZ2A$_{WT}$, H/F-BAZ2A$_{WY/GA}$, and H/F-BAZ2A$_{\Delta TAM}$. BAZ2A-intercating proteins are visualized in immunoblots with the corresponding antibodies.

E. TOP2A and KDM1A interactions with BAZ2A depend on RNA. HA-immunoprecipitation from nuclear extract of the PC3 cell line expressing endogenous BAZ2A with H/F tag (H/F-BAZ2Aend) and parental PC3 cells that were treated with or without RNase A (0.1µg/µl). BAZ2A-intercating proteins are visualized in immunoblots with the corresponding antibodies.

F. Schema representing the role of BAZ2A-TAM domain and RNA in mediating BAZ2A association with TOP2A, KDM1A, SMC1A, RAD21, and NUP107.

Figure 5

TOP2A and KDM1A expression levels correlate with BAZ2A levels in primary and metastatic PCa.

A,B. Boxplots showing expression profiles of *TOP2A* (**A**) and *KDM1A* (**B**) from gene expression microarray GEO data sets GDS2545 (Chandran et al., 2007; Yu et al., 2004) and GDS1439 (Varambally et al., 2005) . Statistical significance (*P*-value) was calculated using two-tailed t-test (* <0.05, **<0.01, ****<0.0001); ns, not significant.

C. Scatter plot showing *BAZ2A* levels relative to *TOP2A* (left panel) and *KDM1A* (right panel) levels from metastatic prostate tumours. Data set is from (Robinson et al., 2015). Statistical significance was calculated using Spearmann correlation.

D. Box plot showing *TOP2A* (left panel) and *KDM1A* (right panel) levels in metastatic tumours expressing high or low BAZ2A levels. Quartile 1: the top 25% of PCas with the highest BAZ2A expression. Quartile 4: the top 25% of PCas with the lowest BAZ2A levels. Error bars represent s.d. Statistical significance (*P*-values) for the experiments was calculated using two-tailed t-test (*** < 0.001).

E. Scatter plot showing *BAZ2A* levels relative to *TOP2A* (left panel) and *KDM1A* (right panel) levels from primary prostate tumours. Data set is from (Cancer Genome Atlas Research, 2015). Statistical significance was calculated using Spearmann correlation.

F. Box plot showing *TOP2A* (left panel) and *KDM1A* (right panel) levels in primary tumours expressing high or low BAZ2A levels. Quartile 1: the top 25% of PCas with the highest BAZ2A expression. Quartile 4: the top 25% of PCas with the lowest BAZ2A levels. Error bars represent s.d. Statistical significance (*P*-values) for the experiments was calculated using two-tailed t-test (*** < 0.001).

G. PCa subtypes and *PTEN* copy number alterations (can) in primary PCa groups defined by BAZ2A, TOP2A, and KDM1A expression levels. Quartile 1 (Q1): the top 25% of PCas with the highest expression. Quartile 4 (Q4): the top 25% of PCas with the lowest levels. The molecular subtypes of primary PCa (ERG fusions, ETV1/ETV4/FLI1 fusions, or overexpression, and SPOP/FOXA1/IDH1 mutations) defined in (Cancer Genome Atlas Research, 2015) are shown.

Figure 6

Downregulation of BAZ2A-TAM repressed genes correlates with tumours expressing high levels of KDM1a and TOP2A

A. Pie chart (top panel) showing the number of genes significantly downregulated by comparing highly and low BAZ2A expressing primary PCas. The number of genes upregulated upon the expression of $BAZ2A_{\Delta TAM}$ in PC3 cells is shown. The pie chart below shows the number of genes that are significantly downregulated in $BAZ2A^{high}/KDM1A^{high}$ tumours compared to $BAZ2A^{low}/KDM1A^{low}$ tumours.

B. Heatmap of log_2 fold change expression levels of BAZ2A-TAM repressed genes downregulated in $BAZ2A^{high}$ vs. $BAZ2A^{low}$ PCas and their corresponding log_2 fold change expression in $BAZ2A^{high}/KDM1A^{high}$ tumours compared to $BAZ2A^{low}/KDM1A^{low}$ tumours.

C. Pie chart (top panel) is the same as in **6A.** The pie chart below shows the number of genes that are significantly downregulated in $BAZ2A^{high}/TOP2A^{high}$ tumours compared to $BAZ2A^{low}/TOP2A^{low}$ tumours.

D. Heatmap of log_2 fold change expression levels of BAZ2A-TAM repressed genes downregulated in $BAZ2A^{high}$ vs. $BAZ2A^{low}$ PCa and their corresponding log_2 fold change expression in $BAZ2A^{high}/TOP2A^{high}$ tumours compared to $BAZ2A^{low}/TOP2A^{low}$ tumours.

E. Proportional venn diagram showing $BAZ2A_{TAM}$ repressed genes downregulated in both $BAZ2A^{high}/KDM1A^{high}$ and $BAZ2A^{high}/TOP2A^{high}$ primary PCas.

F. Box plots showing expression levels (RPKM) of $BAZ2A_{TAM}$ repressed genes downregulated in both $BAZ2A^{high}/KDM1A^{high}$ and $BAZ2A^{high}/TOP2A^{high}$ primary PCas. Error bars represent s.d. Statistical significance (*P*-values) for the experiments was calculated using two-tailed t-test (** < 0.01; *** < 0.001; **** < 0.0001).

G. Pie charts showing the proportion of $BAZ2A_{TAM}$ repressed genes downregulated in both $BAZ2A^{high}/KDM1A^{high}$ and $BAZ2A^{high}/TOP2A^{high}$ primary PCas that are upregulated, downregulated, and non-significantly changed (NS) in metastatic tumours compared to normal tissue. Data set (GDS2545) are from (Chandran et al., 2007; Yu et al., 2004).

H. Boxplots showing expression profiles of $BAZ2A_{TAM}$ repressed genes downregulated in both $BAZ2A^{high}/KDM1A^{high}$ and $BAZ2A^{high}/TOP2A^{high}$ primary and metastatic PCas. Data set (GDS2545) are from (Chandran et al., 2007; Yu et al., 2004). Error bars represent s.d. Statistical significance (*P*-value) was calculated using two-tailed t-test (* <0.05, **<0.01, *** < 0.001, **** < 0.0001); ns, not significant).

Figure 7

KDM1A and TOP2A regulates BAZ2A-TAM dependent genes in PCa cells

A. KDM1A regulates gene expression in PC3 cells. MA plot of the log_2 fold change (FC) gene expression of PC3 cells treated with KDM1Ai OG-L002. Gene expression values of three

replicates were averaged. Blue points represent upregulated genes ($log_2FC > 0.58$) and red points show downregulated genes ($log_2FC < -0.58$) and *P* value < 0.05.

B. Top 10 gene ontology (GO) terms as determined using DAVID for genes upregulated and downregulated in PC3 cells treated with KDM1Ai.

C. Pie chart showing the number of genes significantly upregulated upon $BAZ2A_{\Delta TAM}$ expression in PC3 cells that are affected upon KDM1Ai treatment. The middle panel shows the heat map of log_2 fold change expression levels of genes upregulated by $BAZ2A_{\Delta TAM}$ and affected by KDM1Ai. The right panel shows the number of BAZ2A-TAM repressed and KDM1A-regulated genes that are significantly up- and downregulated upon KDM1Ai treatment.

D. Proportional venn diagram showing the number of upregulated genes by $BAZ2A_{\Delta TAM}$ and KDM1Ai that are downregulated in $BAZ2A^{high}$/$KDM1A^{high}$ primary PCas.

E. TOP2A regulates gene expression in PC3 cells. MA plot of the log_2 fold change (FC) gene expression of PC3 cells treated with TOP2Ai ICR-193. Gene expression values of three replicates were averaged. Blue points represent upregulated genes ($log_2FC > 0.58$) and red points show downregulated genes ($log_2FC < -0.58$) and *P* value < 0.05.

F. Top 10 gene ontology (GO) terms as determined using DAVID for genes upregulated and downregulated in PC3 cells treated with TOP2Ai.

G. Pie chart showing the number of genes significantly upregulated upon $BAZ2A_{\Delta TAM}$ expression in PC3 cells that are affected upon TOP2Ai treatment. Right panel shows the number of BAZ2A-TAM repressed and TOP2A-regulated genes that are up- and downregulated upon TOP2Ai treatment.

H. Proportional venn diagram showing the number of upregulated genes by $BAZ2A_{\Delta TAM}$ and TOP2Ai that are downregulated in $BAZ2A^{high}$/$TOP2A^{high}$ primary PCas.

I. The number of genes upregulated upon $BAZ2A_{\Delta TAM}$ expression and TOP2Ai treatment that are significantly upregulated and downregulated upon KDM1Ai treatment.

J. qRT-PCR showing 45S pre-rRNA levels upon treatment of PC3 cells with KDM1Ai or TOP2Ai. RNA levels were normalized to *GAPDH* mRNA and control cells treated with DMSO. Error bars represent standard deviation of three independent samples. Statistical significance (*P*-value) was calculated using two-tailed t-test. ns, not significant.

Figure 8

KDM1A and TOP2A repress genes that have their inactive C2- enhancers bound by BAZ2A

A. A schema showing the upregulation of genes in the linear nearest proximity to BAZ2A-bound C2-enhancers that are upregulated upon $BAZ2A_{\Delta TAM}$ expression. The pie chart shows the number BAZ2A-TAM dependent C2-enhancer genes that are significantly affected upon KDM1Ai treatment. In the right panel, it is shown the number of BAZ2A-TAM dependent C2-enhancer genes significantly up- and downregulated upon KDM1Ai treatment.

B. The pie chart shows the number BAZ2A-TAM dependent C2-enhancer genes that are significantly affected upon TOP2Ai treatment. In the right panel, it is shown the number of BAZ2A-TAM dependent C2-enhancer genes upregulated by TOP2Ai that are significantly up- and downregulated upon KDM1Ai treatment.

C. Schema representing the role of BAZ2A-TAM, BAZ2A-bromodomain (BRD) and RNA in mediating targeting to C2-enhancers containing H3K14ac and the association with either TOP2A and KDM1A or both for the repression of gene expression in PCa cells.

Supplementary Figures

Supplementary Figure S1

Sample distances dendrogram of three $BAZ2A_{WT}$ samples (WT#1-3) and three $BAZ2A_{\Delta TAM}$ samples (ΔTAM#1-3) using Euclidean distance of the log_2-transformed counts from RNAseq. Dark colour indicates higher correlation between the samples.

Supplementary Figure S2

Boxplots showing expression profiles of genes were linked to signal transduction, response to wounding and cell migration and motility that are repressed through BAZ2A-TAM domain from the gene expression microarray GEO data set GDS2545 (Chandran et al., 2007; Yu et al., 2004). Statistical significance (*P*-value) was calculated using two-tailed t-test (*<0.05, **<0.01, ***< 0.001, ****<0.0001); ns, not significant.

Supplementary Figure S3

A. Left panel. Quantifications of primary $BAZ2A^{high}$ and $BAZ2A^{low}$ Pcas and the expression levels of KDM1A. Right panel. Quantifications of primary $KDM1A^{high}$ and $KDM1A^{low}$ Pcas and the expression levels of BAZ2A. Quartile 1 (Q1): the top 25% of Pcas with the highest expression. Quartile 4 (Q4): the top 25% of Pcas with the lowest levels.

B. Left panel. Quantifications of primary $BAZ2A^{high}$ and $BAZ2A^{low}$ Pcas and the expression levels of TOP2A. Right panel. Quantifications of primary $TOP2A^{high}$ and $TOP2A^{low}$ Pcas and the expression levels of BAZ2A.

C. Left panel. Quantifications of primary $BAZ2A^{high}/KDM1A^{high}$and $BAZ2A^{low}/KDM1A^{low}$ Pcas and the expression levels of TOP2A. Right panel. Quantifications of primary $BAZ2A^{high}/TOP2A^{high}$and $BAZ2A^{low}/TOP2A^{low}$ Pcas and the expression levels of KDM1A.

D. Top gene ontology (GO) terms as determined using DAVID for genes downregulated in primary Pcas $BAZ2A^{high}/KDM1A^{high}$ and $BAZ2A^{high}/TOP2A^{high}$.

E. Top gene ontology (GO) terms as determined using DAVID for genes downregulated in metastatic PCas $BAZ2A^{high}/KDM1A^{high}$ and $BAZ2A^{high}/TOP2A^{high}$.

Supplementary Figure S4

A. Pie chart showing the number of genes significantly downregulated upon BAZ2A$_{\Delta TAM}$ expression in PC3 cells. In the middle panel is shown the heat map of log_2 fold change expression levels of genes downregulated by BAZ2A$_{\Delta TAM}$ and affected by KDM1Ai. In the right panel is shown the number of these genes that are significantly up- and downregulated by KDM1Ai.

B. Pie chart showing the number of genes significantly downregulated upon BAZ2A$_{\Delta TAM}$ expression in PC3 cells that are affected upon TOP2Ai treatment. Middle panel shows the number of genes downregulated by BAZ2A$_{\Delta TAM}$ and regulated by TOP2A that are up- and downregulated upon TOP2Ai treatment. The right panel shows the number of genes downregulated upon BAZ2A$_{\Delta TAM}$ expression and TOP2Ai treatment that are upregulated and downregulated upon KDM1Ai treatment.

Figure 1

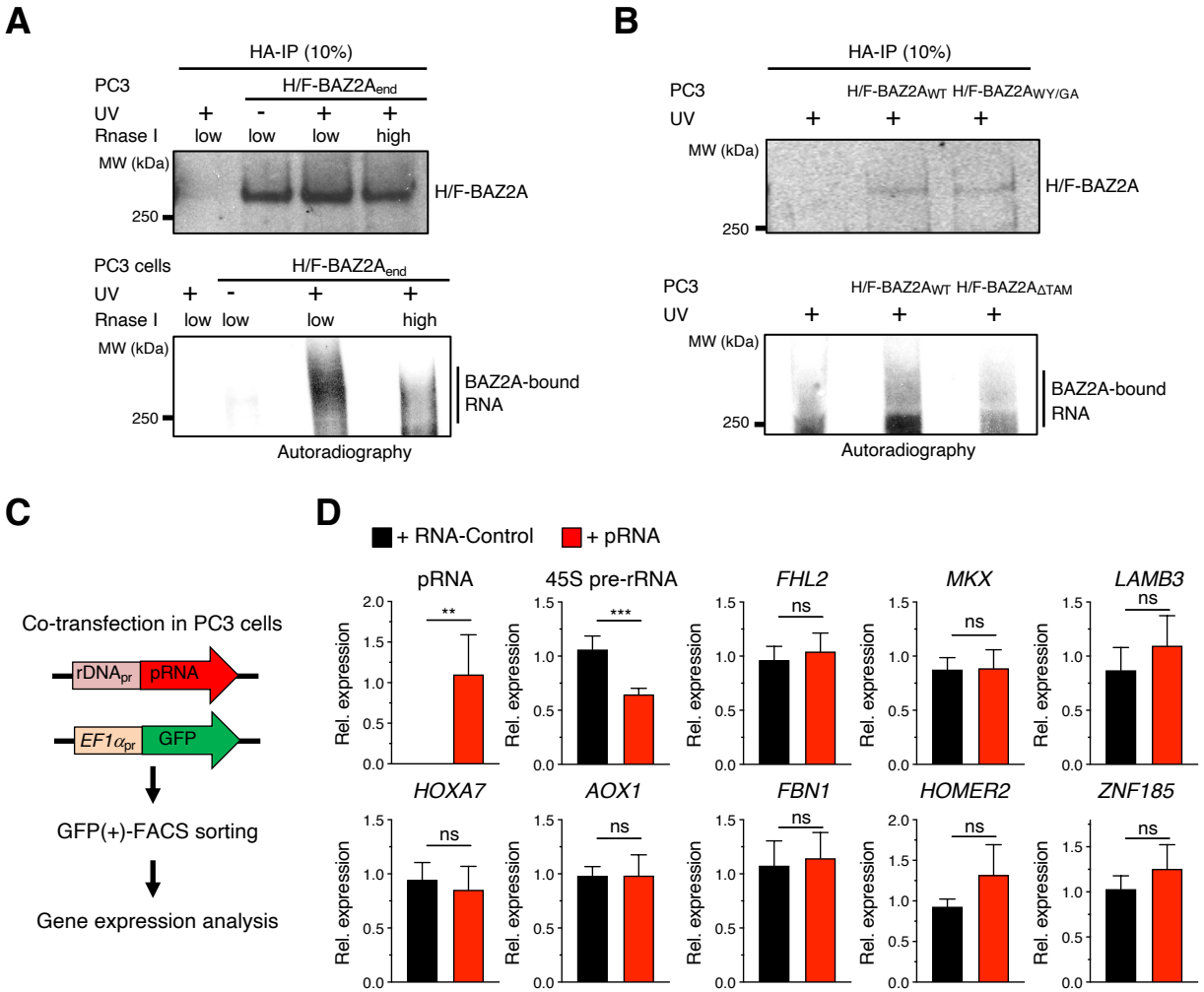
A
HA-IP (10%)
PC3
H/F-BAZ2A$_{end}$
UV
+
-
+
+
Rnase I
low
low
low
high
MW (kDa)
250
H/F-BAZ2A
PC3 cells
H/F-BAZ2A$_{end}$
UV
+
-
+
+
Rnase I
low
low
low
high
MW (kDa)
250
BAZ2A-bound RNA
Autoradiography
B
HA-IP (10%)
PC3
H/F-BAZ2A$_{WT}$
H/F-BAZ2A$_{WY/GA}$
UV
+
+
+
MW (kDa)
250
H/F-BAZ2A
PC3
H/F-BAZ2A$_{WT}$
H/F-BAZ2A$_{\Delta TAM}$
UV
+
+
+
MW (kDa)
250
BAZ2A-bound RNA
Autoradiography
C
Co-transfection in PC3 cells
rDNA$_{pr}$
pRNA
EF1α_{pr}
GFP
GFP(+)-FACS sorting
Gene expression analysis
D
+ RNA-Control
+ pRNA
pRNA
45S pre-rRNA
FHL2
MKX
LAMB3
HOXA7
AOX1
FBN1
HOMER2
ZNF185
Rel. expression
**
***
ns

Figure 2

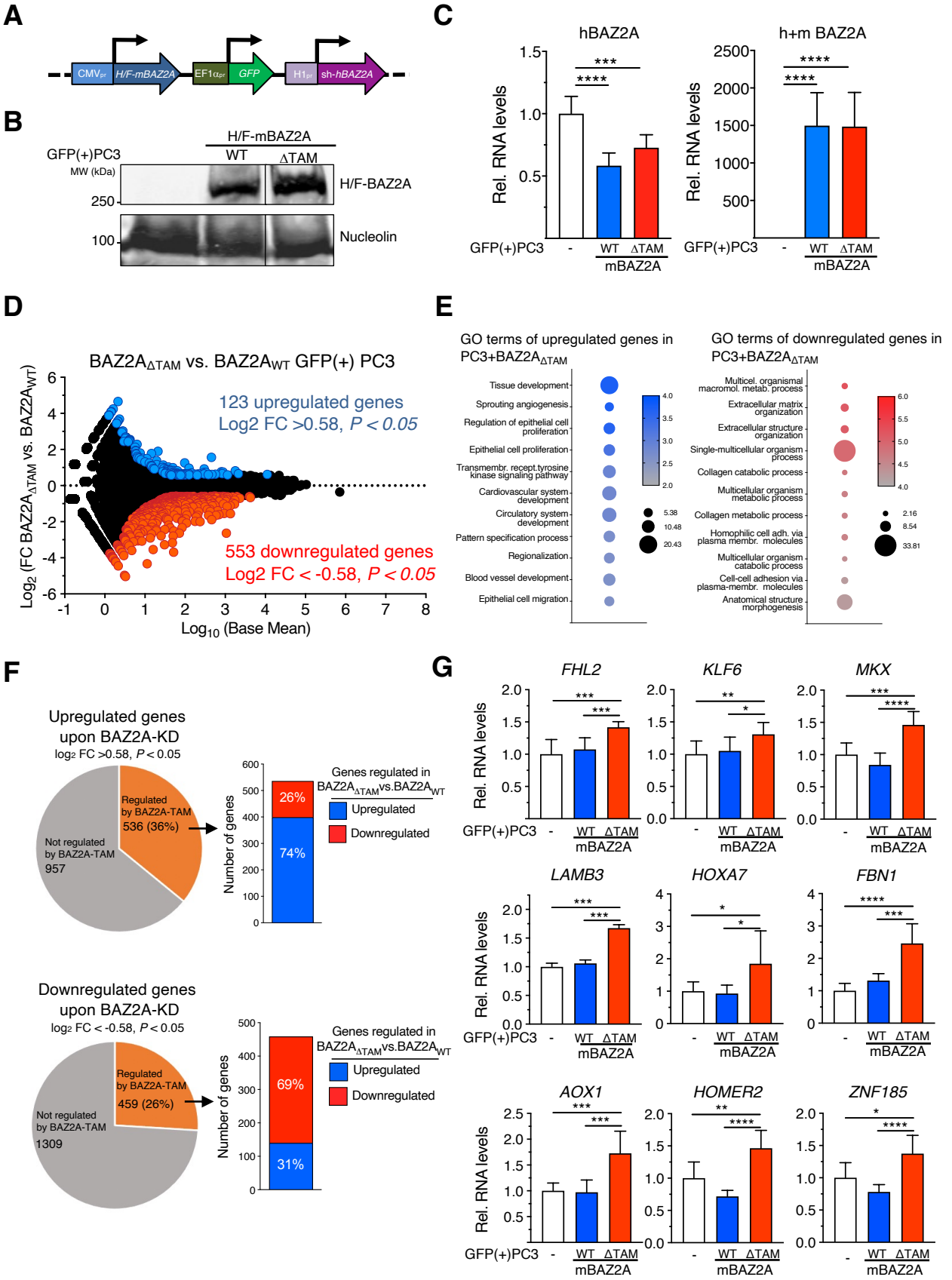
A
CMVpr
H/F-mBAZ2A
EF1αpr
GFP
H1pr
sh-hBAZ2A
B
H/F-mBAZ2A
GFP(+)PC3
WT
ΔTAM
MW (kDa)
250
100
H/F-BAZ2A
Nucleolin
C
hBAZ2A
h+m BAZ2A
Rel. RNA levels
GFP(+)PC3
WT
ΔTAM
mBAZ2A
D
BAZ2AΔTAM vs. BAZ2AWT GFP(+) PC3
123 upregulated genes
Log2 FC >0.58, P < 0.05
553 downregulated genes
Log2 FC < -0.58, P < 0.05
Log2 (FC BAZ2AΔTAM vs. BAZ2AWT)
Log10 (Base Mean)
E
GO terms of upregulated genes in PC3+BAZ2AΔTAM
Tissue development
Sprouting angiogenesis
Regulation of epithelial cell proliferation
Epithelial cell proliferation
Transmembr. recept.tyrosine kinase signaling pathway
Cardiovascular system development
Circulatory system development
Pattern specification process
Regionalization
Blood vessel development
Epithelial cell migration
GO terms of downregulated genes in PC3+BAZ2AΔTAM
Multicel. organismal macromol. metab. process
Extracellular matrix organization
Extracellular structure organization
Single-multicellular organism process
Collagen catabolic process
Multicellular organism metabolic process
Collagen metabolic process
Homophilic cell adh. via plasma membr. molecules
Multicellular organism catabolic process
Cell-cell adhesion via plasma-membr. molecules
Anatomical structure morphogenesis
F
Upregulated genes upon BAZ2A-KD
log2 FC >0.58, P < 0.05
Regulated by BAZ2A-TAM
536 (36%)
Not regulated by BAZ2A-TAM
957
Number of genes
26%
74%
Genes regulated in BAZ2AΔTAM vs.BAZ2AWT
Upregulated
Downregulated
Downregulated genes upon BAZ2A-KD
log2 FC < -0.58, P < 0.05
Regulated by BAZ2A-TAM
459 (26%)
Not regulated by BAZ2A-TAM
1309
69%
31%
G
FHL2
KLF6
MKX
LAMB3
HOXA7
FBN1
AOX1
HOMER2
ZNF185

Figure 3

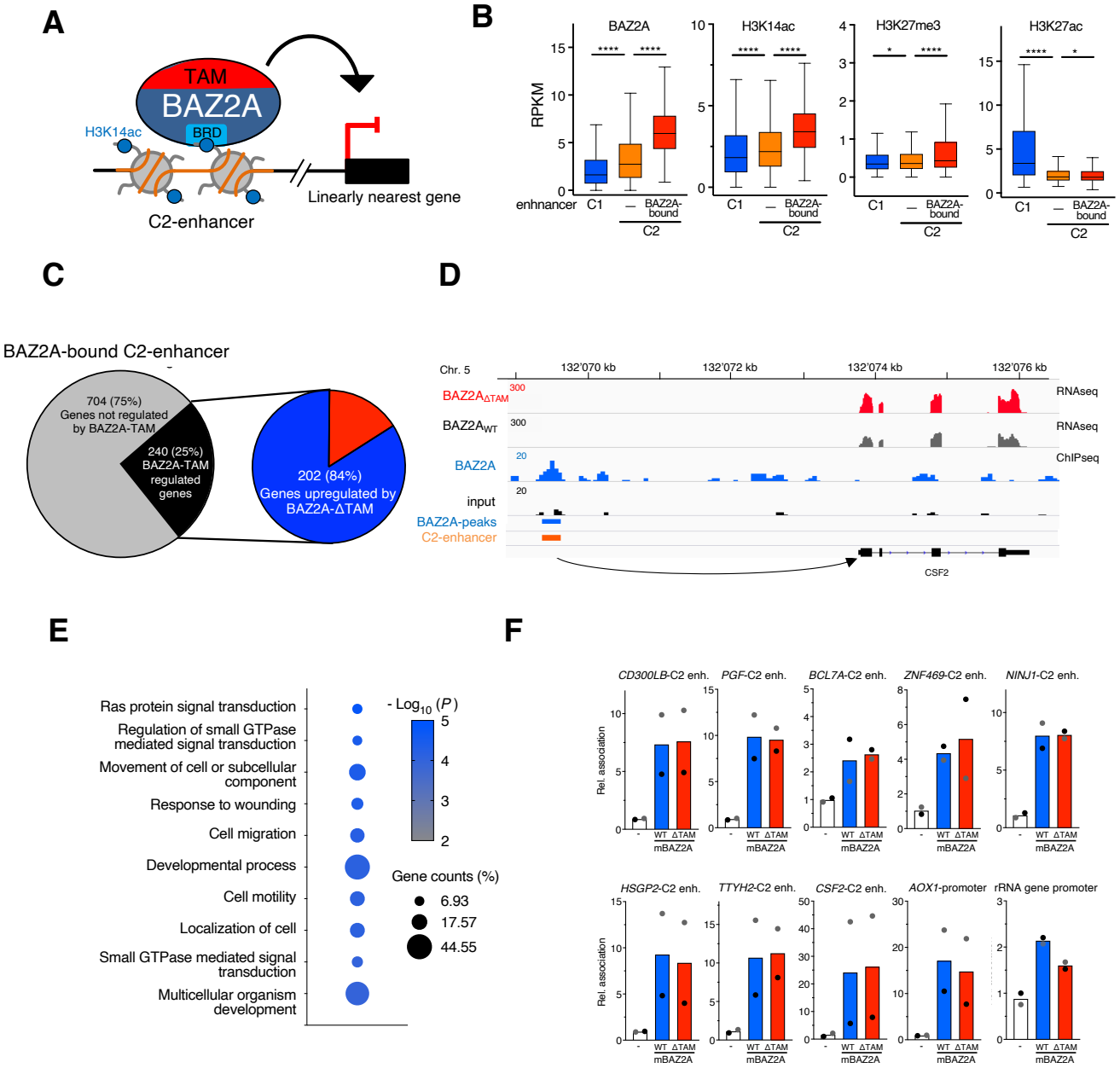
A
TAM
BAZ2A
BRD
H3K14ac
Linearly nearest gene
C2-enhancer
B
BAZ2A
H3K14ac
H3K27me3
H3K27ac
RPKM
enhnancer
C1
BAZ2A-bound
C2
C
BAZ2A-bound C2-enhancer
704 (75%)
Genes not regulated by BAZ2A-TAM
240 (25%)
BAZ2A-TAM regulated genes
202 (84%)
Genes upregulated by BAZ2A-ΔTAM
D
Chr. 5
132'070 kb
132'072 kb
132'074 kb
132'076 kb
BAZ2A$_{\Delta TAM}$
BAZ2A$_{WT}$
BAZ2A
input
BAZ2A-peaks
C2-enhancer
RNAseq
ChIPseq
CSF2
E
Ras protein signal transduction
Regulation of small GTPase mediated signal transduction
Movement of cell or subcellular component
Response to wounding
Cell migration
Developmental process
Cell motility
Localization of cell
Small GTPase mediated signal transduction
Multicellular organism development
- Log$_{10}$ (P)
Gene counts (%)
6.93
17.57
44.55
F
CD300LB-C2 enh.
PGF-C2 enh.
BCL7A-C2 enh.
ZNF469-C2 enh.
NINJ1-C2 enh.
HSGP2-C2 enh.
TTYH2-C2 enh.
CSF2-C2 enh.
AOX1-promoter
rRNA gene promoter
Rel. association
WT
ΔTAM
mBAZ2A

Figure 4

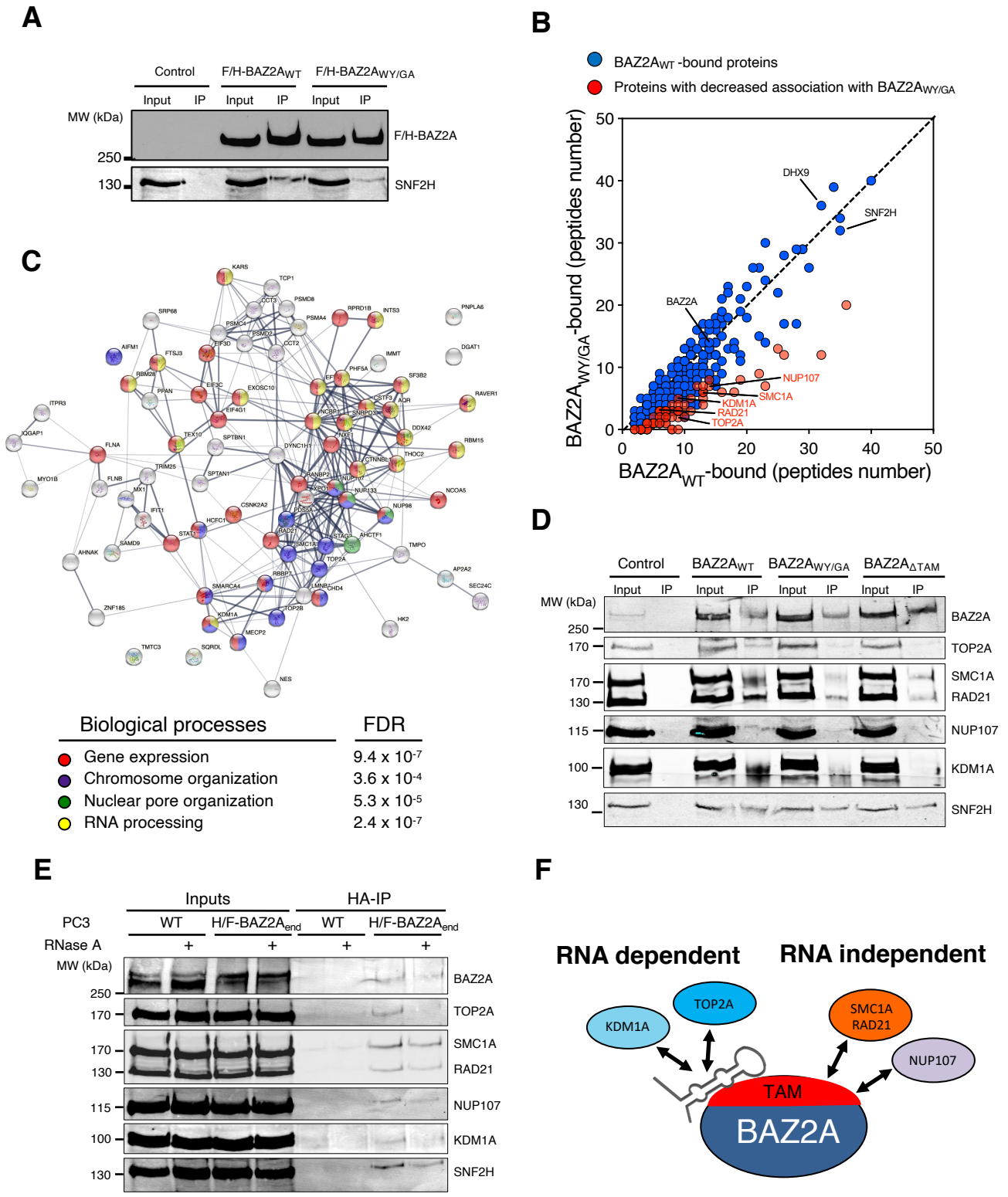
A
Control
F/H-BAZ2A$_{WT}$
F/H-BAZ2A$_{WY/GA}$
Input
IP
MW (kDa)
250
130
F/H-BAZ2A
SNF2H
B
BAZ2A$_{WT}$ -bound proteins
Proteins with decreased association with BAZ2A$_{WY/GA}$
BAZ2A$_{WY/GA}$-bound (peptides number)
BAZ2A$_{WT}$-bound (peptides number)
DHX9
SNF2H
BAZ2A
NUP107
SMC1A
KDM1A
RAD21
TOP2A
C
Biological processes
FDR
Gene expression
9.4 x 10^{-7}
Chromosome organization
3.6 x 10^{-4}
Nuclear pore organization
5.3 x 10^{-5}
RNA processing
2.4 x 10^{-7}
D
Control
BAZ2A$_{WT}$
BAZ2A$_{WY/GA}$
BAZ2A$_{\Delta TAM}$
Input
IP
MW (kDa)
250
170
130
115
100
BAZ2A
TOP2A
SMC1A
RAD21
NUP107
KDM1A
SNF2H
E
Inputs
HA-IP
PC3
WT
H/F-BAZ2A$_{end}$
RNase A
+
MW (kDa)
250
170
130
115
100
BAZ2A
TOP2A
SMC1A
RAD21
NUP107
KDM1A
SNF2H
F
RNA dependent
RNA independent
KDM1A
TOP2A
SMC1A
RAD21
NUP107
TAM
BAZ2A

Figure 5

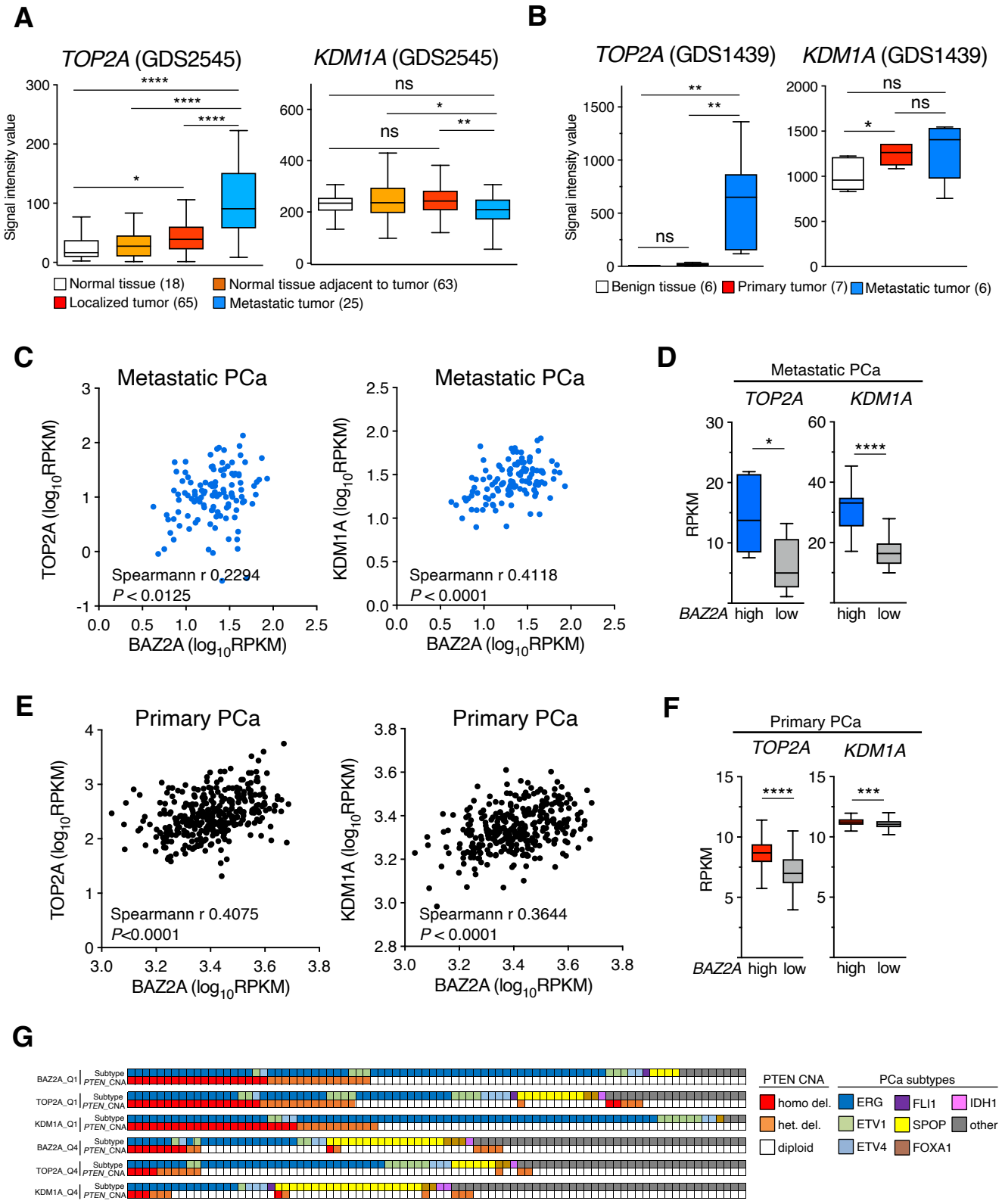
A
TOP2A (GDS2545)
KDM1A (GDS2545)
Signal intensity value
Normal tissue (18)
Normal tissue adjacent to tumor (63)
Localized tumor (65)
Metastatic tumor (25)
B
TOP2A (GDS1439)
KDM1A (GDS1439)
Benign tissue (6)
Primary tumor (7)
Metastatic tumor (6)
C
Metastatic PCa
TOP2A (log10RPKM)
KDM1A (log10RPKM)
BAZ2A (log10RPKM)
Spearmann r 0.2294
P < 0.0125
Spearmann r 0.4118
P < 0.0001
D
Metastatic PCa
TOP2A
KDM1A
RPKM
BAZ2A high low
E
Primary PCa
Spearmann r 0.4075
P<0.0001
Spearmann r 0.3644
P < 0.0001
F
Primary PCa
G
BAZ2A_Q1
TOP2A_Q1
KDM1A_Q1
BAZ2A_Q4
TOP2A_Q4
KDM1A_Q4
Subtype
PTEN_CNA
PTEN CNA
homo del.
het. del.
diploid
PCa subtypes
ERG
FLI1
IDH1
ETV1
SPOP
other
ETV4
FOXA1

Figure 6

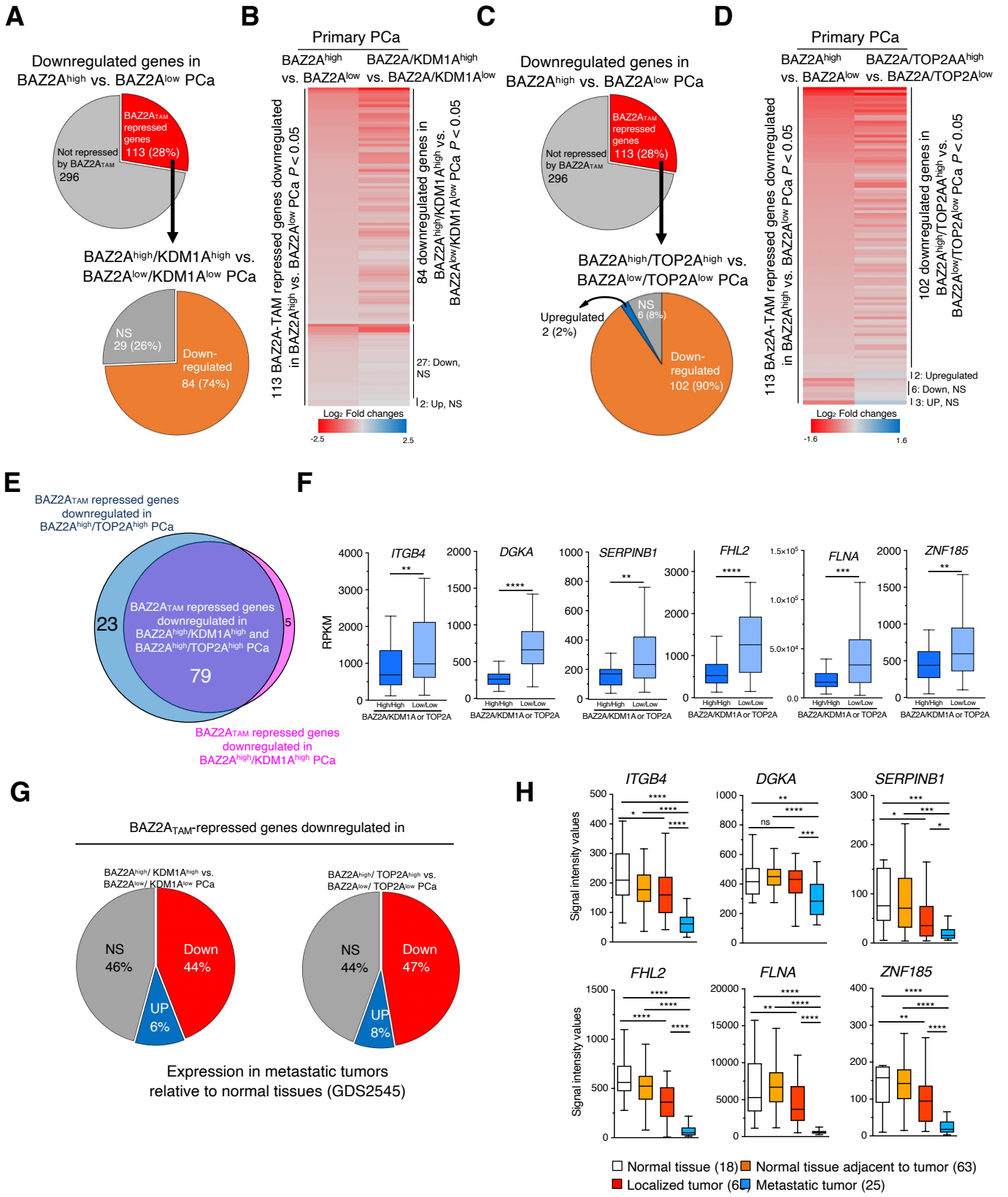
A
Downregulated genes in BAZ2A^{high} vs. BAZ2A^{low} PCa
BAZ2A$_{TAM}$ repressed genes 113 (28%)
Not repressed by BAZ2A$_{TAM}$ 296
BAZ2A^{high}/KDM1A^{high} vs. BAZ2A^{low}/KDM1A^{low} PCa
NS 29 (26%)
Down-regulated 84 (74%)
B
Primary PCa
BAZ2A^{high} vs. BAZ2A^{low}
BAZ2A/KDM1A^{high} vs. BAZ2A/KDM1A^{low}
113 BAZ2A-TAM repressed genes downregulated in BAZ2A^{high} vs. BAZ2A^{low} PCa $P < 0.05$
84 downregulated genes in BAZ2A^{high}/KDM1A^{high} vs. BAZ2A^{low}/KDM1A^{low} PCa $P < 0.05$
27: Down, NS
2: Up, NS
Log$_2$ Fold changes
-2.5
2.5
C
Downregulated genes in BAZ2A^{high} vs. BAZ2A^{low} PCa
BAZ2A$_{TAM}$ repressed genes 113 (28%)
Not repressed by BAZ2A$_{TAM}$ 296
BAZ2A^{high}/TOP2A^{high} vs. BAZ2A^{low}/TOP2A^{low} PCa
Upregulated 2 (2%)
NS 6 (8%)
Down-regulated 102 (90%)
D
Primary PCa
BAZ2A^{high} vs. BAZ2A^{low}
BAZ2A/TOP2AA^{high} vs. BAZ2A/TOP2A^{low}
113 BAz2A-TAM repressed genes downregulated in BAZ2A^{high} vs. BAZ2A^{low} PCa $P < 0.05$
102 downregulated genes in BAZ2A^{high}/TOP2AA^{high} vs. BAZ2A^{low}/TOP2A^{low} PCa $P < 0.05$
2: Upregulated
6: Down, NS
3: UP, NS
Log$_2$ Fold changes
-1.6
1.6
E
BAZ2A$_{TAM}$ repressed genes downregulated in BAZ2A^{high}/TOP2A^{high} PCa
23
BAZ2A$_{TAM}$ repressed genes downregulated in BAZ2A^{high}/KDM1A^{high} and BAZ2A^{high}/TOP2A^{high} PCa
79
5
BAZ2A$_{TAM}$ repressed genes downregulated in BAZ2A^{high}/KDM1A^{high} PCa
F
RPKM
ITGB4
DGKA
SERPINB1
FHL2
FLNA
ZNF185
High/High
Low/Low
BAZ2A/KDM1A or TOP2A
G
BAZ2A$_{TAM}$-repressed genes downregulated in
BAZ2A^{high}/ KDM1A^{high} vs. BAZ2A^{low}/ KDM1A^{low} PCa
NS 46%
Down 44%
UP 6%
BAZ2A^{high}/ TOP2A^{high} vs. BAZ2A^{low}/ TOP2A^{low} PCa
NS 44%
Down 47%
UP 8%
Expression in metastatic tumors relative to normal tissues (GDS2545)
H
ITGB4
DGKA
SERPINB1
FHL2
FLNA
ZNF185
Signal intensity values
Normal tissue (18)
Normal tissue adjacent to tumor (63)
Localized tumor (6
Metastatic tumor (25)

Figure 7

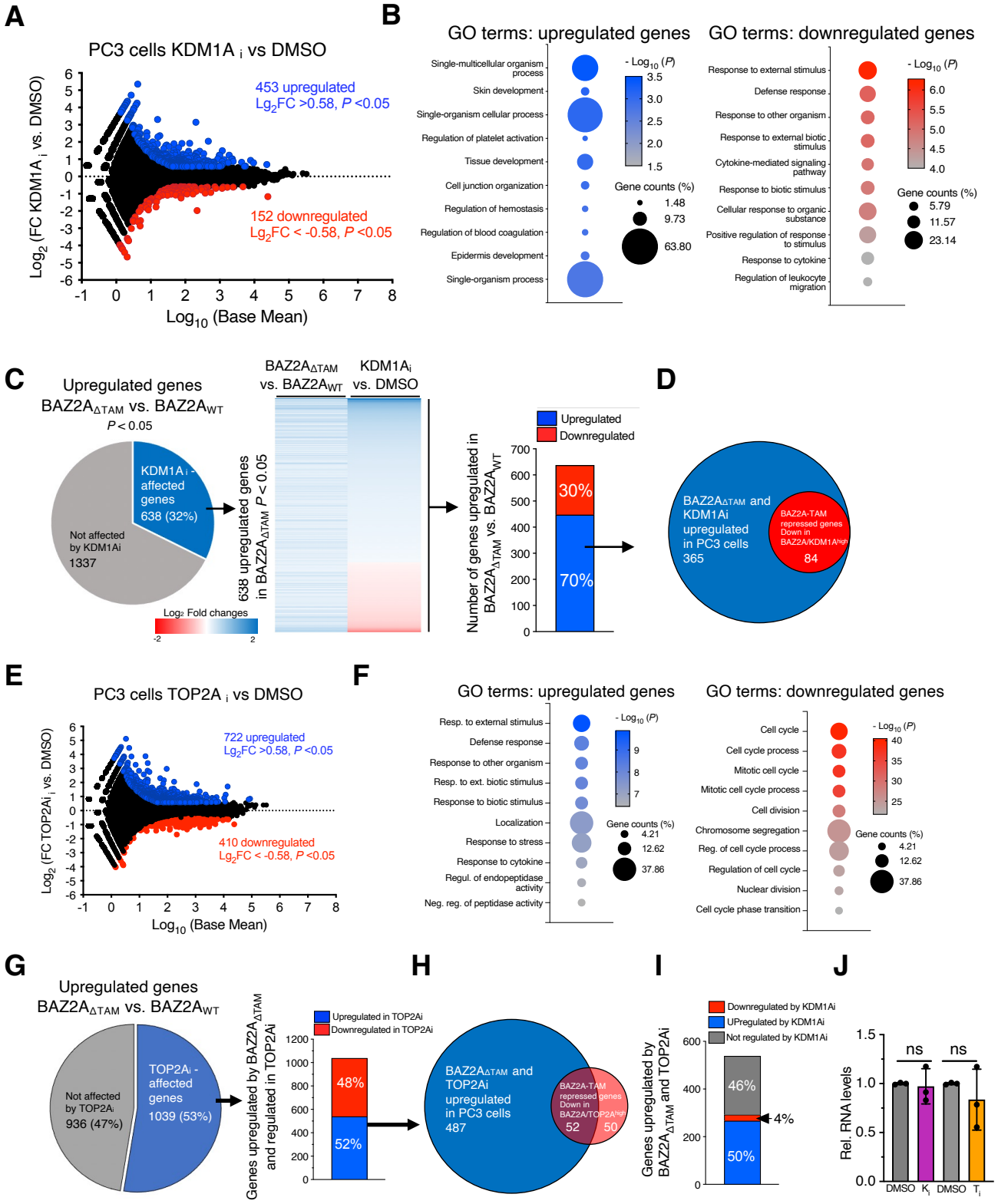
A
PC3 cells KDM1A i vs DMSO
453 upregulated
Lg2FC >0.58, P <0.05
152 downregulated
Lg2FC < -0.58, P <0.05
Log2 (FC KDM1A i vs. DMSO)
Log10 (Base Mean)
B
GO terms: upregulated genes
Single-multicellular organism process
Skin development
Single-organism cellular process
Regulation of platelet activation
Tissue development
Cell junction organization
Regulation of hemostasis
Regulation of blood coagulation
Epidermis development
Single-organism process
- Log10 (P)
Gene counts (%)
GO terms: downregulated genes
Response to external stimulus
Defense response
Response to other organism
Response to external biotic stimulus
Cytokine-mediated signaling pathway
Response to biotic stimulus
Cellular response to organic substance
Positive regulation of response to stimulus
Response to cytokine
Regulation of leukocyte migration
C
Upregulated genes
BAZ2AΔTAM vs. BAZ2AWT
P < 0.05
KDM1A i - affected genes
638 (32%)
Not affected by KDM1Ai
1337
Log2 Fold changes
BAZ2AΔTAM vs. BAZ2AWT
KDM1Ai vs. DMSO
638 upregulated genes in BAZ2AΔTAM P < 0.05
Number of genes upregulated in BAZ2AΔTAM vs. BAZ2AWT
Upregulated
Downregulated
30%
70%
D
BAZ2AΔTAM and KDM1Ai upregulated in PC3 cells
365
BAZ2A-TAM repressed genes Down in BAZ2A/KDM1Ahigh
84
E
PC3 cells TOP2A i vs DMSO
722 upregulated
Lg2FC >0.58, P <0.05
410 downregulated
Lg2FC < -0.58, P <0.05
Log2 (FC TOP2Ai vs. DMSO)
Log10 (Base Mean)
F
GO terms: upregulated genes
Resp. to external stimulus
Defense response
Response to other organism
Resp. to ext. biotic stimulus
Response to biotic stimulus
Localization
Response to stress
Response to cytokine
Regul. of endopeptidase activity
Neg. reg. of peptidase activity
- Log10 (P)
Gene counts (%)
GO terms: downregulated genes
Cell cycle
Cell cycle process
Mitotic cell cycle
Mitotic cell cycle process
Cell division
Chromosome segregation
Reg. of cell cycle process
Regulation of cell cycle
Nuclear division
Cell cycle phase transition
G
Upregulated genes
BAZ2AΔTAM vs. BAZ2AWT
Not affected by TOP2Ai
936 (47%)
TOP2Ai - affected genes
1039 (53%)
Genes upregulated by BAZ2AΔTAM and regulated in TOP2Ai
Upregulated in TOP2Ai
Downregulated in TOP2Ai
48%
52%
H
BAZ2AΔTAM and TOP2Ai upregulated in PC3 cells
487
BAZ2A-TAM repressed genes Down in BAZ2A/TOP2Ahigh
52
50
I
Genes upregulated by BAZ2AΔTAM and TOP2Ai
Downregulated by KDM1Ai
UPregulated by KDM1Ai
Not regulated by KDM1Ai
46%
4%
50%
J
Rel. RNA levels
ns
ns
DMSO
Ki
DMSO
Ti

Figure 8

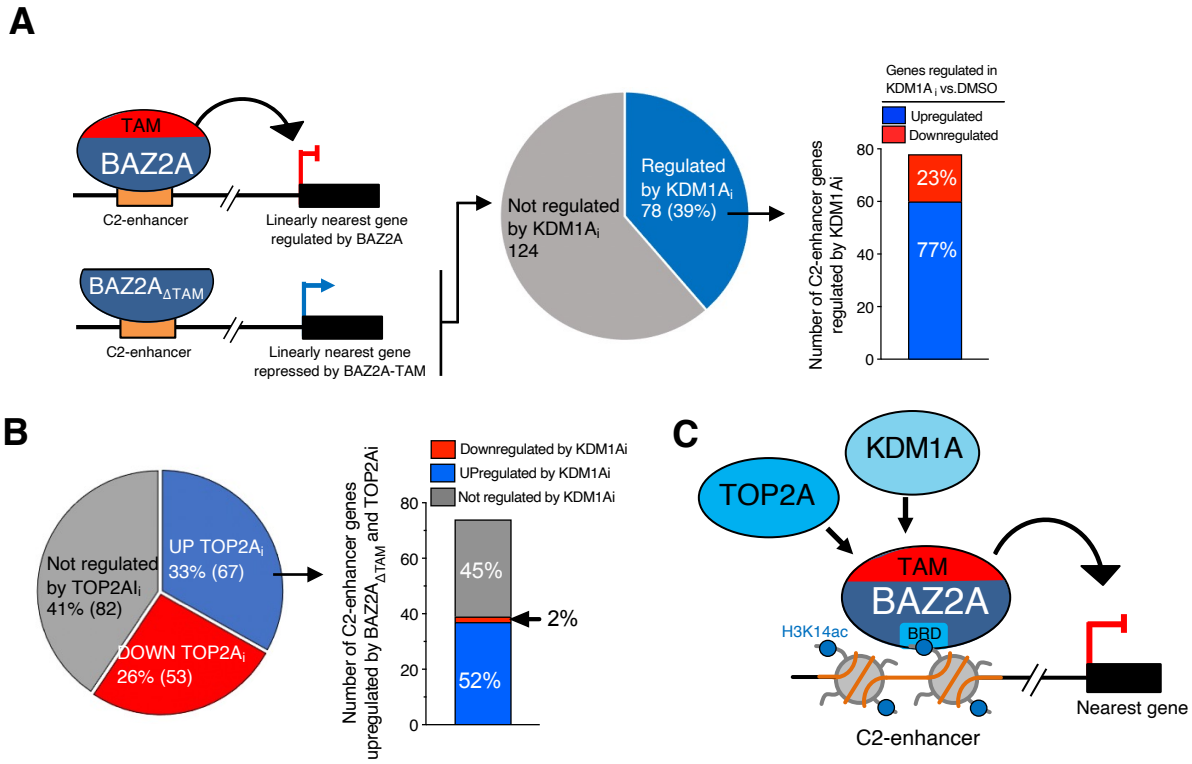
A
TAM
BAZ2A
C2-enhancer
Linearly nearest gene regulated by BAZ2A
BAZ2A$_{\Delta TAM}$
C2-enhancer
Linearly nearest gene repressed by BAZ2A-TAM
Not regulated by KDM1A$_i$ 124
Regulated by KDM1A$_i$ 78 (39%)
Genes regulated in KDM1A$_i$ vs.DMSO
Upregulated
Downregulated
Number of C2-enhancer genes regulated by KDM1Ai
23%
77%
B
Not regulated by TOP2AI$_i$ 41% (82)
UP TOP2A$_i$ 33% (67)
DOWN TOP2A$_i$ 26% (53)
Downregulated by KDM1Ai
UPregulated by KDM1Ai
Not regulated by KDM1Ai
Number of C2-enhancer genes upregulated by BAZ2A$_{\Delta TAM}$ and TOP2Ai
45%
2%
52%
C
TOP2A
KDM1A
TAM
BAZ2A
H3K14ac
BRD
C2-enhancer
Nearest gene